

Cu,Zn-Superoxide Dismutase Increases Toxicity of Mutant and Zinc-deficient Superoxide Dismutase by Enhancing Protein Stability^{*[5]}

Received for publication, March 1, 2010, and in revised form, July 7, 2010. Published, JBC Papers in Press, July 27, 2010, DOI 10.1074/jbc.M110.118901

Mary Anne Sahawneh^{‡§1}, Karina C. Ricart^{¶1||}, Blaine R. Roberts^{**}, Valerie C. Bomben^{‡‡}, Manuela Basso^{‡§}, Yaozu Ye[‡], John Sahawneh[‡], Maria Clara Franco^{‡§2}, Joseph S. Beckman^{**}, and Alvaro G. Estévez^{‡§2,3}

From the [‡]Burke Medical Research Institute, White Plains, New York 10605, the [§]Department of Neurology and Neurosciences, Weill Medical College, New York, New York 10022, the Departments of [¶]Pathology and ^{‡‡}Neurobiology and the ^{||}Center for Free Radical Biology, University of Alabama at Birmingham, Birmingham, Alabama 35294, and the ^{**}Department of Biochemistry and Biophysics, Oregon State University, Corvallis, Oregon 97331

When replete with zinc and copper, amyotrophic lateral sclerosis (ALS)-associated mutant SOD proteins can protect motor neurons in culture from trophic factor deprivation as efficiently as wild-type SOD. However, the removal of zinc from either mutant or wild-type SOD results in apoptosis of motor neurons through a copper- and peroxynitrite-dependent mechanism. It has also been shown that motor neurons isolated from transgenic mice expressing mutant SODs survive well in culture but undergo apoptosis when exposed to nitric oxide via a Fas-dependent mechanism. We combined these two parallel approaches for understanding SOD toxicity in ALS and found that zinc-deficient SOD-induced motor neuron death required Fas activation, whereas the nitric oxide-dependent death of G93A SOD-expressing motor neurons required copper and involved peroxynitrite formation. Surprisingly, motor neuron death doubled when Cu,Zn-SOD protein was either delivered intracellularly to G93A SOD-expressing motor neurons or co-delivered with zinc-deficient SOD to nontransgenic motor neurons. These results could be rationalized by biophysical data showing that heterodimer formation of Cu,Zn-SOD with zinc-deficient SOD prevented the monomerization and subsequent aggregation of zinc-deficient SOD under thiol-reducing conditions. ALS mutant SOD was also stabilized by mutating cysteine 111 to serine, which greatly increased the toxicity of zinc-deficient SOD. Thus, stabilization of ALS mutant SOD by two different approaches augmented its toxicity to motor neurons. Taken together, these results are consistent with copper-containing zinc-deficient SOD being the elusive “partially unfolded intermediate” responsible for the toxic gain of function conferred by ALS mutant SOD.

Mutations to copper/zinc superoxide dismutase (SOD)⁴ are the most common genetic cause of the familial form of amyotrophic lateral sclerosis (ALS) (1, 2). Although transgenic expression of these mutant SOD genes in mice and rats is sufficient to produce a progressive motor neuron disease that mimics human pathology (3), the toxic mechanisms remain obscure. Primary motor neuron cultures have proven to be a powerful model to elucidate the toxic gain of function conferred by ALS mutations to SOD and to determine the underlying cell death pathways. Motor neurons isolated from transgenic mice carrying ALS mutant SOD are fully viable in culture (4, 5) but undergo apoptosis after incubation with low, physiologically relevant concentrations of exogenous nitric oxide (50–100 nM). This remains the most direct evidence that mutant SOD can become directly toxic to motor neurons but also demonstrates that expression of mutant SOD alone may not be sufficient to be toxic to motor neurons.

The concentrations of nitric oxide used to induce death of ALS-SOD-expressing motor neurons were not injurious to motor neurons isolated from transgenic mice expressing wild-type SOD and are even trophic to nontransgenic motor neurons (6). Over the past decade, we have accumulated considerable evidence that the reaction of nitric oxide with superoxide (O₂⁻) to form peroxynitrite (ONOO⁻) is responsible for initiating apoptosis in motor neurons. Superoxide generation can be stimulated in motor neurons by activation of the p75 low affinity neurotrophic receptor, which in turn stimulates a ceramide-dependent pathway (7). Motor neurons themselves can produce sufficient endogenous nitric oxide to activate the death cascade by inducing neuronal nitric-oxide synthase (6, 8, 9). Activation of the Fas receptor strongly up-regulates neuronal nitric-oxide synthase before inducing motor neuron death (4). Alternatively, nitric oxide can also be generated by surrounding cells such as astrocytes in co-culture and diffuse into motor neurons to activate apoptosis. The evidence for superoxide reacting with nitric oxide comes from multiple studies showing that motor neuron death can be prevented

* This work was supported, in whole or in part, by National Institutes of Health Grants NS36761, NS42834 (to A. G. E.), NS058628, AT002034, and ES00240. This work was also supported by funds from the Burke Medical Research Institute, the New York State Spinal Cord Injury Center of Research Excellence, and the Amyotrophic Lateral Sclerosis Association (to J. S. B.).

[5] The on-line version of this article (available at <http://www.jbc.org>) contains supplemental Figs. S1–S3.

¹ Both authors contributed equally to this work.

² Present address: Dept. of Biochemistry and Biophysics, Oregon State University, ALS 2011, Corvallis, OR 97331.

³ To whom correspondence should be addressed. Tel.: 541-737-4517; Fax: 541-737-0481; E-mail: esteveza@onid.orst.edu.

⁴ The abbreviations used are: SOD, superoxide dismutase; ALS, amyotrophic lateral sclerosis; ANOVA, analysis of variance; DETANONOate, (Z)-1-[2-(2-aminoethyl)-N-(2-ammonioethyl)amino]diazene-1-ium-1,2-diolate; MnTBAP, manganese(III) 4,49,40,4-(21H,2H-porphine-5,10,15,20-tetrayl)tetrakis(benzoic acid); FeTCP, iron 5,10,15,20-tetrakis-4-carboxyphenylporphyrin.

Dimer Stabilization Enhances Zinc-deficient SOD Toxicity

either by superoxide scavengers, inhibitors of nitric oxide synthesis, or peroxynitrite scavengers (6, 9–11). In addition, tyrosine nitration, a biomarker of peroxynitrite formation, closely correlates with motor neuron death and is prevented by the same compounds that inhibit the activation of the death cascades (5, 8, 10, 12). We have recently shown that nitration mediated by peroxynitrite may be directly involved in activating motor neuron death (12). Tyrosine nitration has been found in the spinal cord of both transgenic models of ALS and in its human victims (13–17).

As the most efficient scavenger of superoxide in the cytoplasm, Cu,Zn-SOD is an important defense against peroxynitrite-induced motor neuron death. Delivery of Cu,Zn-SOD intracellularly into cultured motor neurons protects them from death induced by trophic factor deprivation. Notably, the intracellular release of eight different ALS mutant Cu,Zn-SODs was found to be just as protective as Cu,Zn-SOD^{WT} in preventing motor neuron death induced by trophic factor deprivation (11). Metal binding to the SOD protein is essential for its biological function. Many mutant SODs bind copper and zinc and maintain full superoxide scavenging activity when expressed as recombinant proteins or *in vivo* (18, 19). However, ALS mutant SODs have a 5–50-fold lower affinity for zinc than the wild-type enzyme (20, 21). Copper remains tightly bound, favoring the formation of zinc-deficient SOD. The loss of zinc disorganizes two loops that form the active site, leaving the copper more accessible to cellular molecules and able to catalyze adverse oxidative reactions including tyrosine nitration (11, 22). We previously showed that zinc-deficient SOD induces a peroxynitrite-dependent death cascade in motor neurons that closely paralleled trophic factor deprivation (11). The primary distinction was that the toxicity of zinc-deficient SOD could be prevented by the copper chelators neocuproine and bathocuproine, whereas these compounds do not protect non-transgenic motor neurons from death induced by trophic factor withdrawal.

Although overexpression of wild-type Cu,Zn-SOD (SOD^{WT}) in animal models generally provides protection against cerebral ischemia and excitotoxicity (23, 24), recent studies have shown that SOD^{WT} increases mutant SOD toxicity *in vivo* (25–27), even in the SOD^{G85R} transgenic mice (28), although it was previously reported that the expression of Cu,Zn-SOD^{WT} had no effect on disease progression in a different SOD^{G85R} line (29). The mechanism for how co-expression of Cu,Zn-SOD^{WT} increases the toxicity of mutant SOD is controversial, with some groups arguing that aggregation plays a role (27, 30) and with others concluding that increased solubility of the enzyme contributes to the enhanced toxicity (26, 31, 32).

Understanding the basis for early onset and faster disease progression is important because the vast majority of familial SOD patients are heterozygotes, and the SOD mutations generally exhibit dominant inheritance. Here, we used motor neurons isolated for ALS mutant-expressing rats and mice to investigate whether the death cascade induced by nitric oxide was similar to that induced by intracellular delivery of zinc-deficient SOD. The investigation was extended to determine whether subunits of Cu,Zn-SOD can increase the toxic gain-of-function of mutant SOD as well as the toxicity of zinc-deficient SOD.

MATERIALS AND METHODS

Isolation of Motor Neurons—Motor neurons were prepared as described previously (8, 33). Briefly, isolated ventral spinal cords from embryonic day 15 rat embryos were trypsinized, and the tissue was disaggregated by trituration. The cell suspension was centrifuged on top of a 6% OptiPrep cushion (Sigma), and the motor neurons were removed from the interface. Motor neurons were further purified by magnet-assisted cell separation (Miltenyi Biotec, Auburn, CA) using the IgG 192 antibody against p75 low affinity neurotrophin receptor (Chemicon-Millipore, Billerica, MA). Motor neurons were plated on 4- or 96-well plates coated with poly-DL-ornithine and laminin (Sigma) at a density of 1500 and 500 cells/well, respectively. The motor neurons were maintained in NeurobasalTM medium supplemented with B27, heat-inactivated horse serum, glutamine, glutamate, 2-mercaptoethanol (all from Invitrogen), and trophic factors (1 ng/ml brain-derived neurotrophic factor, 0.1 ng/ml glial-derived neurotrophic factor, 10 ng/ml cardiotrophin-1) and incubated in a 5% CO₂ humidified atmosphere at 37 °C.

Treatment of Motor Neurons with SOD—SOD was delivered utilizing either Chariot (Active Motif, Carlsbad, CA) or pH-sensitive liposomes. Cu,Zn-SOD or zinc-deficient SOD was diluted in sterile H₂O at a final concentration of 5 µg/ml at room temperature. If Cu,Zn-SOD and zinc-deficient SOD were added together, they were incubated at room temperature for 30 min to allow heterodimer formation. Chariot (3.75 µl/ml) was diluted in H₂O and added to the SOD protein for 30 min to allow complexes to form. After 24 h in culture, the medium was aspirated and replaced with 100 µl of Opti-MEM transfection medium at 37 °C (Invitrogen) containing the mixture Chariot and SOD to be delivered. The cells were incubated at 37 °C for 1 h, at which time 100 µl of 2× NeurobasalTM medium (Invitrogen) plus or minus trophic factors was added to each well and then further incubated for 24 h at 37 °C.

Liposomes were prepared by extrusion using an extruder from Lipex Biomembranes Inc. (Vancouver, Canada), as described (10). Briefly, dioleoylphosphatidyl-ethanolamine (35 µmol) and dioleoylglycero succinate (35 µmol; Avanti Polar Lipids, Alabaster, AL) were dried under nitrogen followed by vacuum and then hydrated with 1 ml of 210 mM sucrose in 7 mM HEPES, pH 8.5, for 24–48 h at 37 °C. Human SOD (5 mg in 50 µl) was added to 250 µl of the hydrated lipids. The mixture was vortexed, and the extrusion was performed for 10–15 cycles through a 0.6-µm Nucleopore membrane (Millipore Corp., Bedford, MA). The liposomes were centrifuged at 150,000 × *g* for 1 h, rinsed once with fresh sucrose-HEPES buffer, and resuspended in 250 µl of the same solution. Typically 2.5–3 mg of SOD were incorporated into liposomes, and 1 µl of liposomes were added per well, which corresponds to 50 nmol of lipids and 10 µg of SOD. The liposomes were added to 24-h-old motor neuron cultures after replacing the culture medium with fresh NeurobasalTM containing B27 supplement, glutamine, 2-mercaptoethanol, and the corresponding trophic factors. Horse serum and glutamate were omitted from the medium.

Immunofluorescence—The motor neurons were stained as described previously (8). Briefly, the medium was removed and

replaced with L15 plus 4% paraformaldehyde for 2 min on ice. The cells were rinsed three times with L15 and incubated for 20 min with 4% paraformaldehyde. After rinsing, the slides were incubated with 50 mM lysine, 0.1% Triton X-100 in PBS for 15 min at room temperature. The cells were blocked using 5% BSA at room temperature for 1 h. Primary antibodies were incubated in blocking solution in a humidified chamber at 4 °C overnight and rinsed three times for 5 min with PBS. Fluorescent secondary antibodies were added in blocking solution for 1 h at room temperature protected from light. The cells were rinsed three times for 5 min with PBS and with water once before being mounted using ProLong Gold with 4',6-diamidino-2-phenylindole (Molecular Probes-Invitrogen).

Motor Neuron Survival—Motor neuron survival was determined either by counting cells with neurites longer than four soma diameters under a phase contrast microscope in four-well plates as described previously (8) or by high throughput image capture and analysis in 96-well plates using a Flash Cytometer™ (Trophos, Marseilles, France) as reported before (34). For high throughput image capture, motor neurons plated in black 96-well plates coated with poly-D-ornithine and laminin (Greiner Bio-one, Monroe, NC) were treated with calcein-AM (Molecular Probes-Invitrogen) in L15 medium (Invitrogen) for 1 h at 37 °C. Fifteen μl /well of 100 mg/ml of hemoglobin in PBS was added to quench extracellular calcein, and the plates were read using a Flash Cytometer. Cell counts were obtained and are represented as percentages of survival relative to the survival in the presence of neurotrophic factors (1 ng/ml brain-derived neurotrophic factor, 0.1 ng/ml glial-derived neurotrophic factor, and 10 ng/ml cardiotrophin-1) used as 100% survival to standardize between experiments as described previously (8). Image analysis was performed using the Tina™ software (Trophos) or the Metamorph™ software (Molecular Devices, Downingtown, PA). The results for the different treatments were equivalent using liposomes or Chariot and either method of quantifying motor neuron survival.

Kinetics of SOD Dimer Formation—Sedimentation velocity ultracentrifugation experiments were performed in a Beckman Optima XL-A analytical ultracentrifuge as described previously (22). Buffer densities and viscosity corrections were made as described previously (35). The protein sequence was used to estimate the partial specific volume of SOD ($0.725 \text{ cm}^3 \text{ g}^{-1}$) (22, 36). Sedimentation velocity centrifugation was performed at 20 °C using an AN-60Ti rotor and double-sector charcoal/Epon-filled centerpieces. SOD samples ($10 \mu\text{M}$, $A_{230} = 0.8$) were centrifuged at 42,000 rpm. Typically, three 360- μl samples of $20 \mu\text{M}$ SOD (or $10 \mu\text{M}$ Cu,Zn-SOD plus $10 \mu\text{M}$ zinc-deficient D124N SOD) were centrifuged. Scans were collected with absorbance optics at wavelengths between 230 and 280 nm. The radial step size was 0.001 cm, and each *c versus r* data point was the average of 15 independent measurements. Wavelengths were chosen such that the absorbance never exceeded 1.0. Using UltraScan software, equilibrium data were fit to multiple models using global fitting. The most appropriate model was chosen based on the goodness-of-fit and inspection of the residual patterns.

Gel filtration experiments were performed by incubating SOD for 1 or 24 h with increasing concentrations of DTT

(0–100 mM). To ensure that the DTT was fully reduced, tributylphosphine ($100 \mu\text{l}$) was added to 0.5 M DTT ($400 \mu\text{l}$). The solution was mixed gently, and then 1-bromo-3-chloropropane ($100 \mu\text{l}$) was added. The reduced DTT was collected after separation into an upper phase. The concentration of SOD used was $20 \mu\text{M}$ for all cases, whereas the heterodimer samples consisted of $10 \mu\text{M}$ zinc-deficient D83S/C111S SOD plus $10 \mu\text{M}$ wild-type Cu,Zn-SOD. After incubation for either 1 or 24 h at room temperature, the samples were separated using a TosoHaas™ G3000SWXL column with 100 mM NaPO_4 , pH 7.0, as the running buffer and a flow rate of 1.0 ml/min. Elution of protein was monitored at 214 nm, and the percentage of monomer was determined by dividing the area of the monomer by the total area of dimer and monomer.

Statistical Analysis—The statistical analysis was performed using Prism™ 5.0b software (GraphPad Software, Inc.). Multiple comparisons were performed using one- or two-way ANOVA, depending on the experimental design, followed by post-hoc test. In specific groups that did not pass the homoscedasticity test, the statistical analysis was performed using the Kruskal-Wallis test. The values were considered significantly different when $p < 0.05$. Dose-response curves were fitted to a sigmoid curve when possible using nonlinear regression without restrictions. All of the experiments were repeated at least three times with each condition performed at least in duplicate in each experiments.

RESULTS

Copper Chelation Protects Motor Neurons Expressing ALS Mutant SOD^{G93A} from Death Induced by Nitric Oxide—Motor neurons isolated from G93A transgenic rats (37) were exposed to low steady state concentrations of nitric oxide ($\sim 100 \text{ nM}$) produced by the nitric oxide donor DETANONOate ($20 \mu\text{M}$) for 24 h in the presence or absence of the specific Cu^{1+} chelator bathocuproine ($50 \mu\text{M}$). Bathocuproine significantly reversed SOD^{G93A} transgenic motor neuron death induced by nitric oxide (Fig. 1A). The metalloporphyrin peroxynitrite and superoxide scavengers MnTBAP ($100 \mu\text{M}$) and FeTCPP ($10 \mu\text{M}$) both prevented nitric oxide-induced transgenic motor neuron death (Fig. 1A). Similar results were obtained using motor neurons isolated from SOD^{G93A} transgenic mice (not shown). Incubation of motor neurons carrying the G93A SOD mutation with exogenous nitric oxide showed increased nitrotyrosine immunoreactivity, which was reversed by treatment with bathocuproine or with MnTBAP (Fig. 1B).

Cu,Zn-SOD Increases the Toxic Effect of Nitric Oxide on G93A Mutant SOD Transgenic Motor Neurons—To further test the role of superoxide on nitric oxide toxicity, Cu,Zn-SOD^{WT} ($1 \mu\text{g}$) was released intracellularly into motor neurons from SOD^{G93A} transgenic as well as nontransgenic rat motor neurons. SOD was delivered with the membrane-permeating agent Chariot, and the treated motor neurons were also incubated with the nitric oxide donor DETANONOate ($20 \mu\text{M}$). The intracellular delivery of SOD protein into motor neurons was verified by immunofluorescence (supplemental Fig. S1). The prediction of the experiment was that if superoxide was involved, Cu,Zn-SOD should protect against nitric oxide-induced toxicity in transgenic motor neurons. Paradoxically,

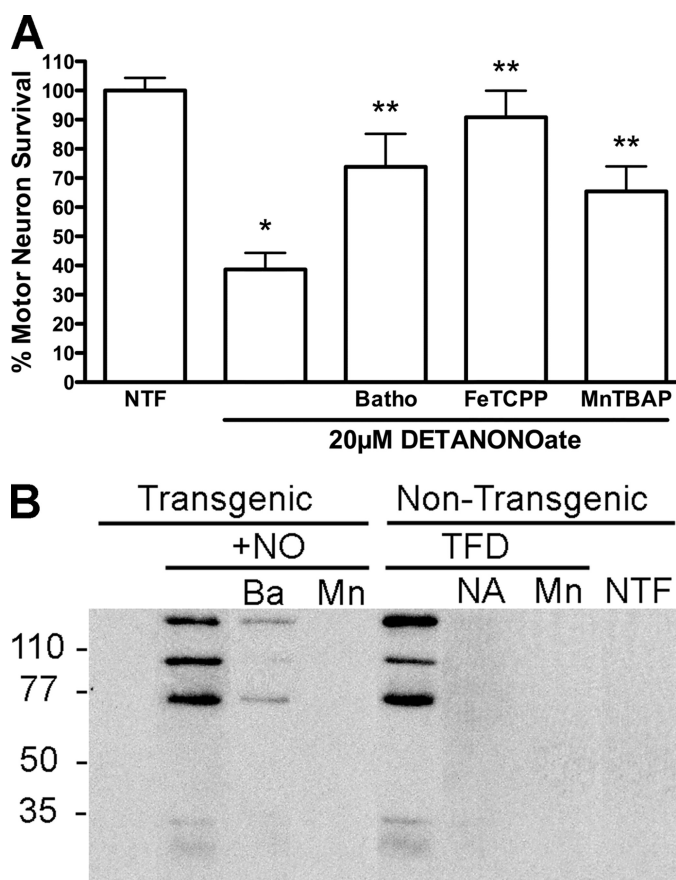


FIGURE 1. A, SOD^{G93A} motor neurons are protected by superoxide scavengers. Motor neurons isolated for G93A transgenic rats were plated in four-well plates and incubated with and without the nitric oxide donor DETANONOate (20 μM) for 24 h in the presence of trophic factors (NTF). At the time of plating the copper chelator, bathocuproine (50 μM; Batho) and the superoxide and peroxynitrite scavengers FeTCPP (10 μM) and MnTBAP (100 μM) were added to the culture medium. The values are the means ± S.D. of at least three independent experiments performed in quadruplicate. Statistical analysis was performed using the Kruskal-Wallis test followed by Dunn's multiple comparison test. *, *p* < 0.05 versus NTF. **, *p* < 0.05 versus DETANONOate. B, nitrotyrosine formation after incubation of transgenic motor neurons with exogenous nitric oxide. Enriched motor neurons prepared from transgenic rats carrying the G93A SOD mutant or nontransgenic littermates by density centrifugation (motor neuron purity higher than 80%) were plated in 35-mm dishes at a density of 75,000 cells/dish as described before. Twenty-four hours after plating the cultures of transgenic motor neurons were incubated with DETANONOate (+NO, 20 μM) alone or in combination with bathocuproine (Ba; 5 μM) or MnTBAP (Mn; 100 μM) for 16 h. Nontransgenic motor neurons were incubated in the presence (NTF) or absence (TFD) of neurotrophic factors for 16 h. Trophic factor-deprived motor neurons were incubated alone or with L-NAME (NA; 100 μM) and MnTBAP (Mn; 100 μM). Protein was harvested, and 100 μg of protein was separated per lane using SDS-PAGE. After transferring the proteins to a PVDF membrane, the nitrotyrosine was visualized using a monoclonal antibody to nitrotyrosine as described previously (12).

intracellular delivery of Cu,Zn-SOD^{WT} enhanced nitric oxide-induced transgenic motor neuron death in a dose-dependent manner but had no effect on motor neuron survival in the absence of nitric oxide (Fig. 2A). SOD added to the medium without Chariot, intracellular release of apoSOD, BSA, or copper-loaded BSA did not affect motor neuron survival, whether or not the cells were exposed to nitric oxide (not shown). In agreement with previous reports (5, 8, 10, 38), nitric oxide did not decrease survival of nontransgenic motor neurons even with intracellular delivery of Cu,Zn-SOD^{WT} (Fig. 2B). Conversely, scavenging of superoxide and peroxynitrite with

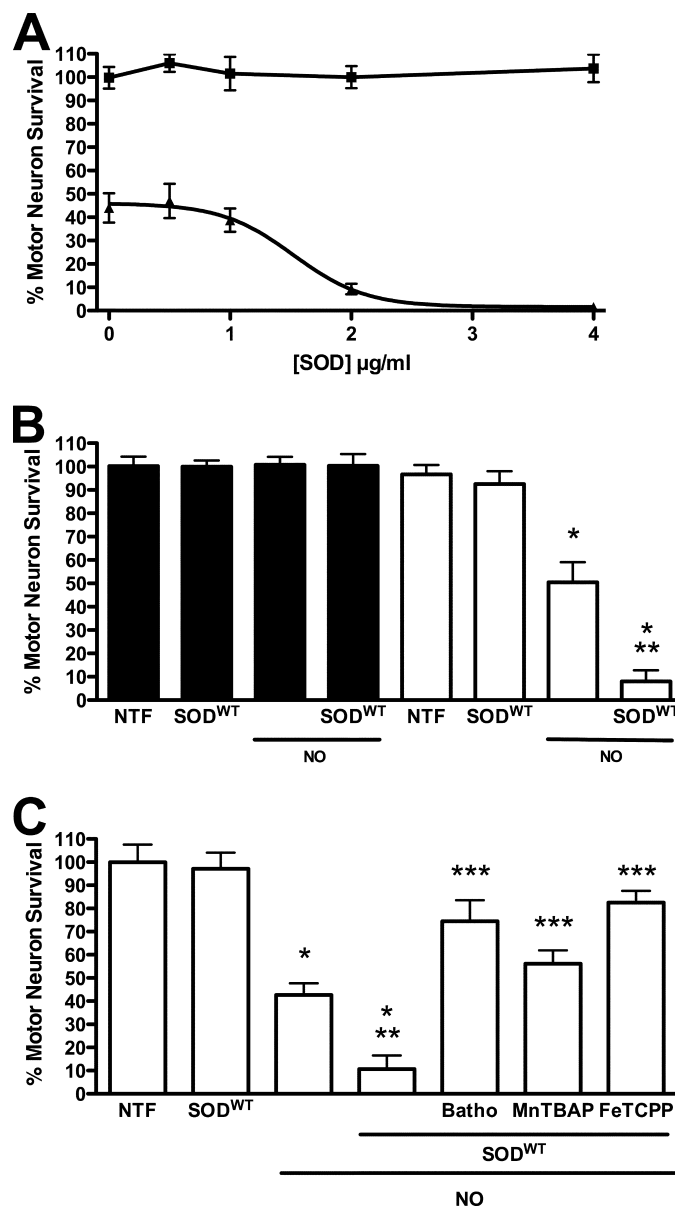


FIGURE 2. Cu,Zn-SOD^{WT} enhances nitric oxide-induced SOD^{G93A} motor neuron death. Motor neurons purified from transgenic rat for SOD^{G93A} and nontransgenic littermates were plated in four-well plates and treated as indicated, and survival was determined 24 h later. A, motor neurons from transgenic rats for SOD^{G93A} were incubated with growing concentrations of Cu,Zn-SOD^{WT} alone (■) or in combination with DETANONOate (20 μM) (▲). The values representing the means ± S.D. of at least three independent experiments performed in duplicate were fitted to a sigmoid curve with EC₅₀ = 1.5 ± 0.15 μg (95% confidence interval (C.I.) 1.20 to 1.80) and R² = 0.934. B, motor neurons isolated from SOD^{G93A} (open bars) and from nontransgenic littermates (filled bars) were incubated with 20 μM DETANONOate (NO), Cu,Zn-SOD^{WT} (1 μg), or the combination of both treatments. The values are the means ± S.D. of at least three independent experiments performed in quadruplicate. The values were analyzed by two-way ANOVA followed by Bonferroni's multiple comparison test. *, *p* < 0.01 versus transgenic NTF. **, *p* < 0.01 versus transgenic incubated with NO alone. C, motor neurons from transgenic rat were incubated with SOD^{WT} released using Chariot, alone or in combination with 20 μM DETANONOate (NO). Cultures treated with SOD^{WT} and DETANONOate were also incubated with the copper chelator bathocuproine (50 μM, Batho), and the superoxide and peroxynitrite scavengers MnTBAP (100 μM) and FeTCPP (10 μM). The values are the means ± S.D. of three independent experiments performed in duplicate. The values were analyzed by ANOVA followed of Bonferroni's multiple comparison test. *, *p* < 0.05 versus NTF. **, *p* < 0.05 versus NO alone. ***, *p* < 0.05 versus NO plus SOD.

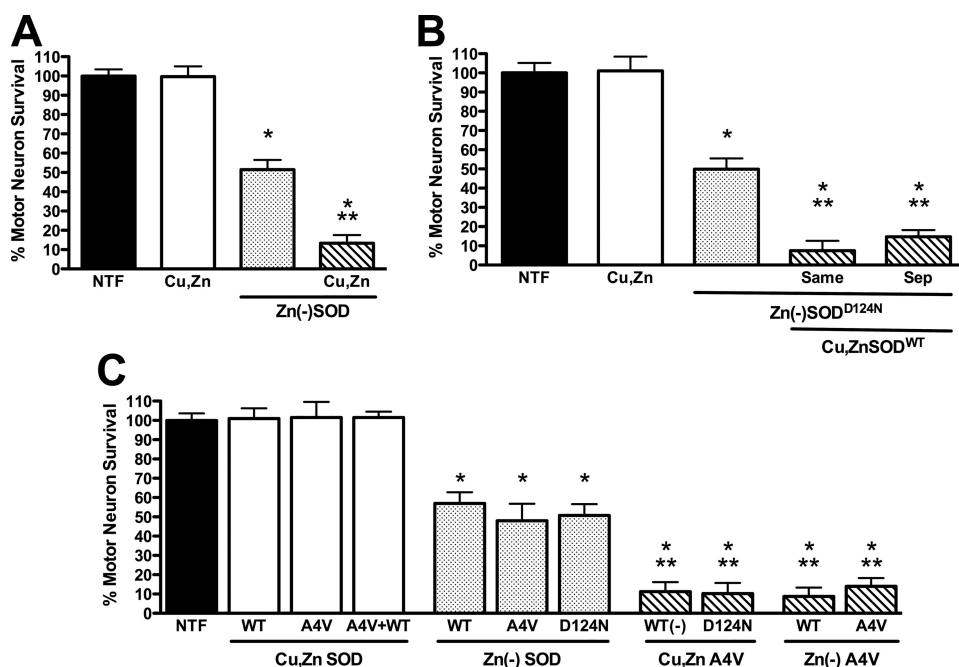


FIGURE 3. Cu,Zn-SOD enhances zinc-deficient SOD toxicity. Rat motor neurons were plated in four-well plates and incubated for 24 h in the presence of trophic factors (NTF) before any treatment. The addition of zinc-deficient SOD and Cu,Zn-SOD was performed using pH-sensitive liposomes to motor neurons incubated with trophic factors. *A*, motor neurons were incubated with Cu,Zn-SOD^{WT} (10 μg, Cu,Zn, open bar), zinc-deficient SOD^{WT} (10 μg, Zn(-)SOD, dotted bar), and Cu,Zn-SOD^{WT} (5 μg) plus zinc-deficient SOD^{WT} (5 μg) in separate liposomes (slashed bar). The values are the means ± S.D. of at least three independent experiments each performed in duplicate. The data were analyzed by ANOVA followed by Bonferroni's multiple comparison test. *, *p* < 0.05 versus NTF. **, *p* < 0.05 versus Zn(-)SOD. *B*, motor neurons were incubated with Cu,Zn-SOD^{WT} (10 μg, Cu,Zn, open bar), zinc-deficient SOD^{D124N} (10 μg, Zn(-)SOD, dotted bar), and Cu,Zn-SOD^{WT} (5 μg) plus zinc-deficient SOD^{D124N} (5 μg, slashed bar), and the enzymes were mixed before the preparation of the liposomes and added in the same liposomes (Same) or liposomes for Cu,Zn-SOD^{WT} and zinc-deficient SOD^{D124N} were separately prepared and mixed just before addition to the motor neurons (Sep). The values are the means ± S.D. of at least three independent experiments performed in duplicate. The data were analyzed by ANOVA followed by Bonferroni's multiple comparison test. *, *p* < 0.05 versus NTF. **, *p* < 0.05 versus Zn(-)SOD. *C*, motor neurons were incubated as described previously with Cu,Zn enzyme (10 μg; open bars), zinc-deficient enzyme (10 μg; dotted bars), and a mixture of Cu,Zn (5 μg) and zinc-deficient (5 μg) enzyme prepared in separated liposomes (slashed bars). WT, SOD^{WT}; A4V, SOD^{A4V}; D124N, SOD^{D124N}. (-) indicates zinc-deficient. SOD^{D124N} is a spontaneously low zinc-binding enzyme and in the experiment conditions is zinc-deficient (11). The values are the means ± S.D. of at least three independent experiments performed in duplicate. The data were analyzed by ANOVA followed by Bonferroni's multiple comparison test. *, *p* < 0.05 versus NTF. **, *p* < 0.05 versus zinc-deficient SOD^{A4V}.

MnTBAP (100 μM) and FeTCPP (10 μM) and copper chelation with bathocuproine (50 μM) reversed SOD^{G93A} transgenic motor neuron death induced by nitric oxide plus Cu,Zn-SOD^{WT} (Fig. 2C) to the same extent as with nitric oxide alone (Fig. 1).

Cu,Zn-SOD Increased Zinc-deficient SOD Toxicity on Non-transgenic Motor Neurons—To investigate the effect of Cu,Zn-SOD on zinc-deficient SOD-induced motor neuron death, experiments were performed using pH-sensitive liposomes rather than Chariot to deliver the enzyme (10, 39). The use of liposomes was necessary to prevent the surreptitious binding of zinc to zinc-deficient SOD that would occur in the culture medium if the Chariot method was used (11). Liposomes loaded with 10 μg of either zinc-deficient SOD^{WT}, SOD^{A4V}, or SOD^{D124N} all induced ~50% motor neuron death after 24 h in culture (Fig. 3) as previously reported (11). When half of the zinc-deficient SOD^{WT} was replaced with Cu,Zn-SOD^{WT} (5 μg of each enzyme), motor neuron death increased from ~50% to >85% (Fig. 3A). The enhanced toxicity was independent of whether zinc-deficient SOD^{WT} and Cu,Zn-SOD^{WT} were encapsulated in the same liposome preparation or the zinc-

deficient, and Cu,Zn-SODs were added to cells in separately prepared liposomes (Fig. 3B). The enhanced toxicity was also independent of whether the zinc-deficient SOD was a wild-type or an ALS mutant protein (Fig. 3C). Thus, Cu,Zn-SOD^{A4V} plus zinc-deficient SOD^{WT} was just as toxic as Cu,Zn-SOD^{WT} plus zinc-deficient SOD^{A4V} (Fig. 3C).

The same results were obtained using human SOD in which the aspartate residue in position 83 was mutated to serine (SOD^{D83S}). This mutation disrupts the binding of zinc without affecting the binding of copper (22). Because this mutant protein will not rebind zinc in culture medium, it could be delivered with Chariot. The effects of releasing the zinc-deficient SOD^{D83S} and Cu,Zn-SOD with Chariot were indistinguishable from those using liposomes for intracellular delivery (see Fig. 5 and supplemental Fig. S2).

To determine whether superoxide and peroxynitrite production were necessary for the enhanced toxicity of zinc-deficient SOD in the presence of Cu,Zn-SOD, we investigated the effect of metalloporphyrins on motor neuron survival. Both MnTBAP (100 μM) and FeTCPP (10 μM) reversed motor neuron death induced by trophic factor deprivation, intracellular release of zinc-deficient SOD, and zinc-deficient

SOD plus Cu,Zn-SOD (Fig. 4). These results show that motor neuron death triggered by combining zinc-deficient SOD with Cu,Zn-SOD involved the same mechanism as the enhanced cell death observed when Cu,Zn-SOD was delivered to transgenic SOD^{G93A} motor neurons treated with nitric oxide.

Zinc-deficient SOD Toxicity Is Mediated by Activation of the Fas Pathway—Nitric oxide-induced mutant SOD transgenic motor neuron death requires activation of the Fas death receptor and peroxynitrite production (4, 5). Because copper chelation as well as scavenging of superoxide and peroxynitrite prevented the susceptibility of transgenic mutant SOD motor neurons to nitric oxide as shown in Fig. 1, we asked whether activation of the Fas pathway was necessary for zinc-deficient SOD to induce motor neuron death. Incubation of motor neurons with the Fas receptor decoy Fas:Fc (1 μg/ml) prevented motor neuron death induced by trophic factor deprivation (Fig. 5A), as previously reported (33). The same concentration of Fas:Fc prevented zinc-deficient SOD^{D83S}-induced motor neuron death (Fig. 5B). Furthermore, the enhanced motor neuron death triggered by simultaneous incubation with both zinc-de-

Dimer Stabilization Enhances Zinc-deficient SOD Toxicity

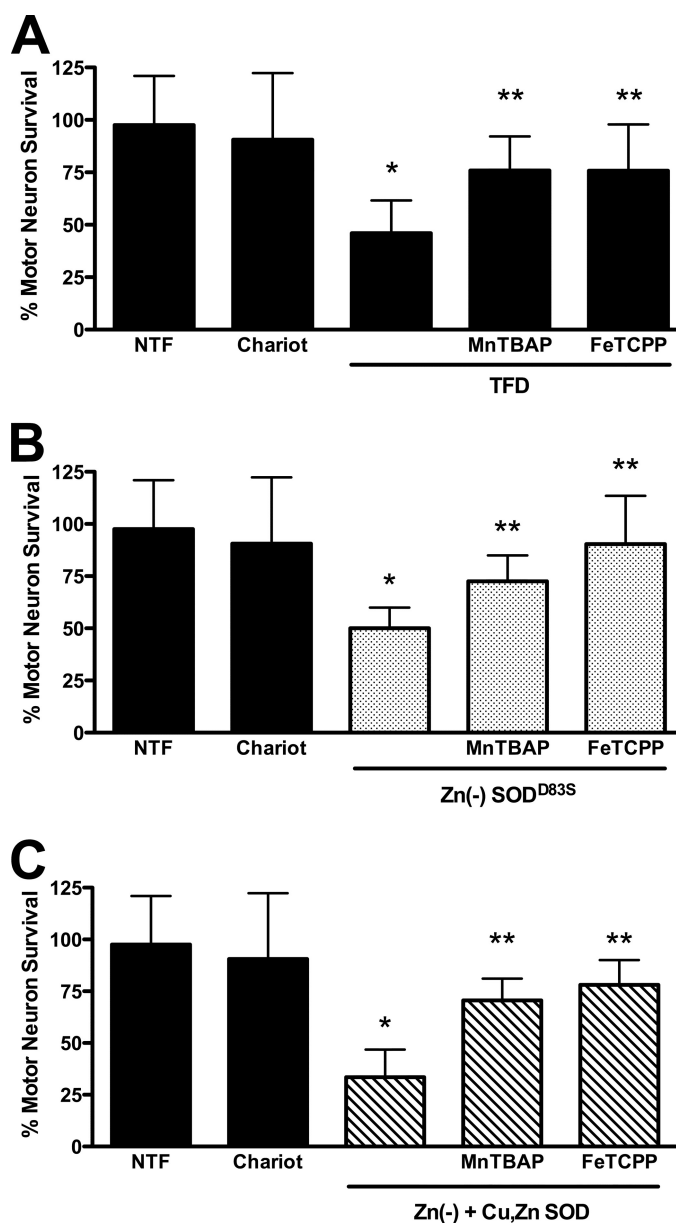


FIGURE 4. Superoxide and peroxynitrite scavengers prevent Cu,Zn-SOD plus zinc-deficient SOD toxicity. Motor neurons were plated in 96-well plates for 24 h before replacing the medium with fresh medium without glutamate, and survival was determined 24 h later by high throughput image capture and analysis. Motor neuron survival was quantified by high throughput image capture and analysis (supplemental Fig. S3). The number of motor neurons in the presence of trophic factors was considered as 100% survival to standardize between experiments. Using this approach, and releasing 1 $\mu\text{g/ml}$ of SOD/well, there were no differences in motor neuron survival as compared with the experiments performed using pH-sensitive liposomes. The incubation of motor neurons with equivalent concentrations of extracellular wild-type, mutant, Cu,Zn, or zinc-deficient SOD in the absence of Chariot had no effect on survival in the presence or absence of trophic factors (not shown). **A**, after replacing the medium, the cultures were incubated with (NTF) or without trophic factors (TFD), and Chariot was added in the presence of trophic factors to determine potential toxicity. Trophic factor-deprived motor neurons were incubated with the superoxide scavengers MnTBAP (100 μM) and FeTCPP (10 μM). The values are the means \pm S.D. of three independent experiments performed eight times. The data were analyzed by ANOVA followed by Bonferroni's multiple comparison test. *, $p < 0.05$ versus NTF. **, $p < 0.05$ versus Chariot. **B**, motor neurons incubated with trophic factors (NTF) were exposed to zinc-deficient SOD^{D835} (1 $\mu\text{g/well}$, Zn(-)SOD^{D835}; dotted bars) in Optitem for 1 h after the addition of complete culture medium supplemented for all the volume. MnTBAP (100 μM) and FeTCPP (10 μM) were added to motor neurons incubated with zinc-deficient SOD. The values are

the means \pm S.D. of three independent experiments performed eight times. The data were analyzed by ANOVA followed by Bonferroni's multiple comparison test. *, $p < 0.05$ versus Chariot. **, $p < 0.05$ versus zinc-deficient SOD^{D835}. **C**, motor neurons incubated with trophic factors (NTF) were exposed to zinc-deficient SOD^{D835} (0.5 $\mu\text{g/well}$) plus Cu,Zn-SOD^{WT} (0.5 $\mu\text{g/well}$; Zn(-) + Cu,ZnSOD; slashed bars) in Optitem for 1 h after the addition of complete culture medium supplemented for all the volume. MnTBAP (100 μM) and FeTCPP (10 μM) were added to motor neurons incubated with the mixture of zinc-deficient and Cu,Zn-SOD. The values are the means \pm S.D. of three independent experiments performed eight times. The data were analyzed by ANOVA followed by Bonferroni's multiple comparison test. *, $p < 0.05$ versus Chariot. **, $p < 0.05$ versus the mixture of zinc-deficient plus Cu,Zn-SOD. Two-way ANOVA analysis followed by Bonferroni's multiple comparison test of the groups in B and C indicate that Zn(-) + Cu,Zn-SOD (C) is significantly different from Zn(-)SOD^{D835} $p < 0.05$.

efficient SOD^{D835} and Cu,Zn-SOD^{WT} was also prevented by incubation with Fas:Fc (Fig. 5C). It has been previously shown that Fas receptor activation in motor neurons leads to phosphorylation and activation of the p38 MAPK, which is necessary for neuronal NOS induction and nitric oxide production (5). Inhibition of p38 MAPK with SB203580 (5 μM) prevented the induction of motor neuron death by zinc-deficient SOD^{D835} and zinc-deficient SOD^{D835} plus Cu,Zn-SOD^{WT} (Fig. 6), which is consistent with the activation of the Fas pathway previously reported in the death of ALS mutant transgenic motor neurons (4, 5). The JNK MAPK pathway has been implicated as an upstream regulator of FasL expression (40). Two structurally different JNK inhibitors, JNK II inhibitor (1 μM) and JNK III inhibitor (1 μM), prevented motor neuron death induced by trophic factor deprivation (Fig. 7A), as expected from previous reports using motor neurons isolated from ALS mutant SOD transgenic mice (5, 41, 42). These same inhibitors prevented motor neuron death induced by zinc-deficient SOD^{D835} (Fig. 7B) and zinc-deficient SOD^{D835} plus Cu,Zn-SOD^{WT} (Fig. 7C).

Nitric Oxide, Peroxynitrite, and Tyrosine Nitration Are Necessary for Zinc-deficient SOD-induced Motor Neuron Death—Activation of the Fas pathway in motor neurons leads to the induction of NOS, nitric oxide production, and peroxynitrite formation (5), as is the case for zinc-deficient SOD (11) and SOD^{G93A} transgenic motor neurons treated with exogenous nitric oxide (4). Inhibition of nitric oxide production with L-NAME protected motor neurons treated with zinc-deficient SOD^{D835} alone (Fig. 8A) or in combination with Cu,Zn-SOD^{WT} (Fig. 8B). The protective effect of L-NAME was abolished by low steady state concentrations of nitric oxide (100 nM) produced by DETANONOate (20 μM), which supports the conclusion that the protection afforded by L-NAME was due to inhibition of nitric oxide production (Fig. 8, A and B).

We have previously shown that tyrosine-containing peptides inhibit peroxynitrite-mediated apoptosis and tyrosine nitration but do not directly scavenge peroxynitrite or prevent thiol oxidation (12). These peptides also do not prevent apoptosis induced by hydrogen peroxide or staurosporine (12). Incubation of motor neurons with the most effective of the nitration-inhibiting peptides RYEYA (0.5 mM) and EYTA (0.5 mM) prevented motor neuron death induced by zinc-deficient SOD^{WT} (Fig. 8C). The same peptides containing phenylalanine (RFEFA or EFTA) were not protective; these analogs were previously shown to not be effective competitive inhibitors of tyrosine nitration (12). These results extend our previous observations

the means \pm S.D. of three independent experiments performed eight times. The data were analyzed by ANOVA followed by Bonferroni's multiple comparison test. *, $p < 0.05$ versus Chariot. **, $p < 0.05$ versus zinc-deficient SOD^{D835}. **C**, motor neurons incubated with trophic factors (NTF) were exposed to zinc-deficient SOD^{D835} (0.5 $\mu\text{g/well}$) plus Cu,Zn-SOD^{WT} (0.5 $\mu\text{g/well}$; Zn(-) + Cu,ZnSOD; slashed bars) in Optitem for 1 h after the addition of complete culture medium supplemented for all the volume. MnTBAP (100 μM) and FeTCPP (10 μM) were added to motor neurons incubated with the mixture of zinc-deficient and Cu,Zn-SOD. The values are the means \pm S.D. of three independent experiments performed eight times. The data were analyzed by ANOVA followed by Bonferroni's multiple comparison test. *, $p < 0.05$ versus Chariot. **, $p < 0.05$ versus the mixture of zinc-deficient plus Cu,Zn-SOD. Two-way ANOVA analysis followed by Bonferroni's multiple comparison test of the groups in B and C indicate that Zn(-) + Cu,Zn-SOD (C) is significantly different from Zn(-)SOD^{D835} $p < 0.05$.

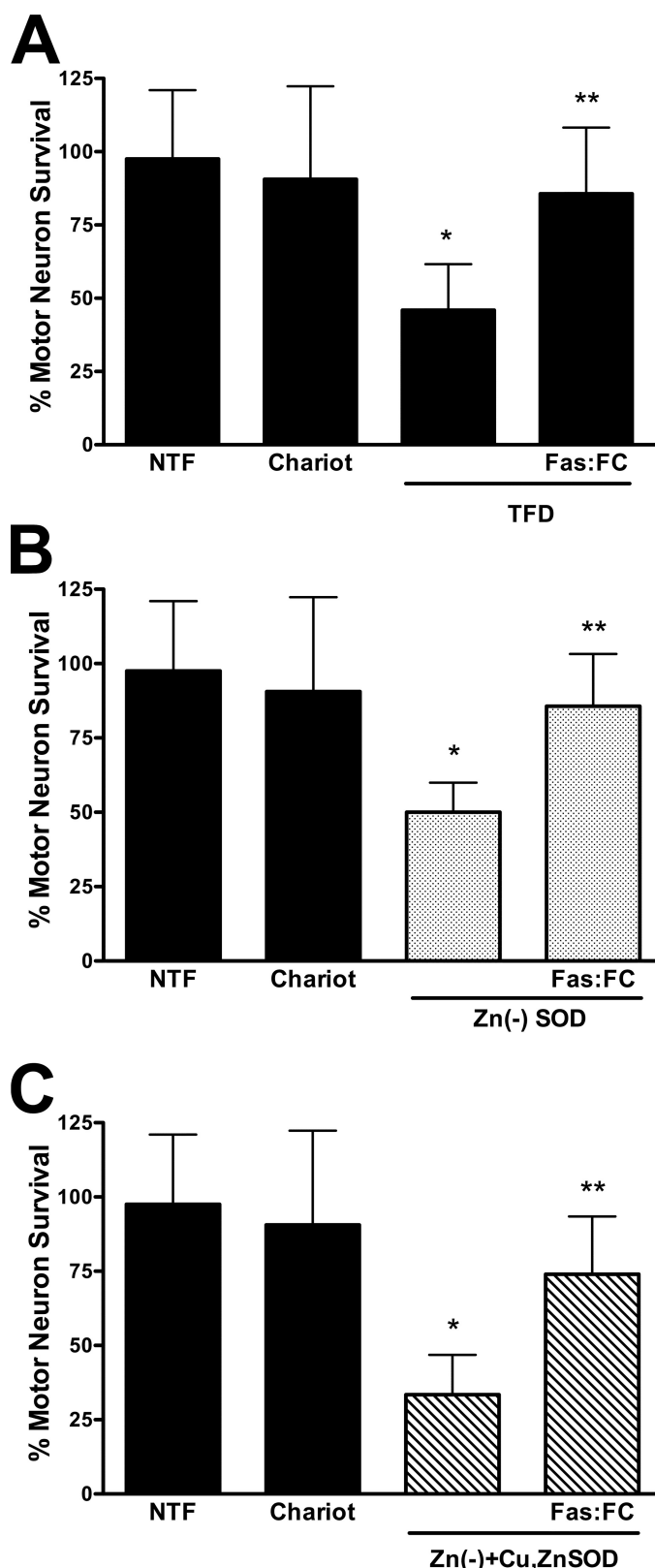


FIGURE 5. Zinc-deficient SOD stimulates Fas-dependent motor neuron death. Motor neurons were plated and treated as described in the legend to Fig. 4. *A*, motor neurons were incubated with trophic factors alone (*NTF*) or with Chariot, without trophic factors (*TFD*), and without trophic factor supplemented with 1 μ g/ml of the Fas ligand decoy Fas:Fc. The values are the means \pm S.D. of three independent experiments performed eight times. The data were analyzed by ANOVA followed by Bonferroni's multiple comparison test. *, $p < 0.05$ versus *NTF*. **, $p < 0.05$ versus *TFD*. *B*, motor neurons were

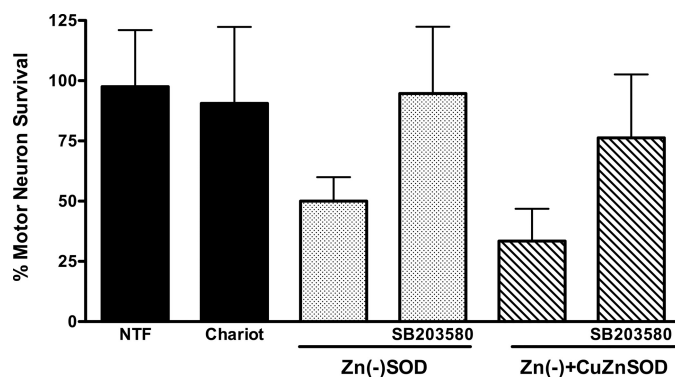


FIGURE 6. Inhibition of p38 MAPK prevented zinc-deficient SOD toxicity. Motor neurons were plated and treated as described in the legend Fig. 4. *A*, motor neurons were incubated with trophic factors (*NTF*) or trophic factors supplemented with Chariot alone or with Chariot plus zinc-deficient SOD^{D835} (1 μ g, Zn(-)SOD; dotted bars) with or without the p38 MAPK inhibitor SB203580 (5 μ M). The values are the means \pm S.D. of three independent experiments performed eight times. The data were analyzed by ANOVA followed by Bonferroni's multiple comparison test. *, $p < 0.05$ versus zinc-deficient SOD^{D835}. *B*, motor neurons were treated as in *A* but with zinc-deficient SOD^{D835} (0.5 μ g) plus Cu,Zn-SOD^{WT} (0.5 μ g; Zn(-)+CuZnSOD; slashed bars). The values are the means \pm S.D. of three independent experiments performed eight times. The data were analyzed by ANOVA followed by Bonferroni's multiple comparison test. *, $p < 0.05$ versus Chariot. **, $p < 0.05$ versus zinc-deficient SOD^{D835} plus Cu,Zn-SOD^{WT}.

that tyrosine nitration plays a role in the induction of motor neuron death by trophic factor deprivation to include death induced by zinc-deficient SOD.

Cu,Zn-SOD Dimers with Zinc-deficient SOD Increases Protein Stability—Zinc-deficient SOD^{D835} forms heterodimers with Cu,Zn-SOD^{WT} subunits with a half-life of 17 min at 37 °C (22). In the absence of a sulfhydryl-reducing agent, both Cu,Zn-SOD^{WT} and zinc-deficient SOD^{D835} existed solely as dimers during sedimentation velocity ultracentrifugation (Fig. 9A). In the presence of the thiol-reducing agent DTT (1 mM), zinc-deficient SOD^{D835} existed as 60% monomer, 30% dimer (30%), and 10% in a dynamic exchange state that was intermediate between monomer and dimer (Fig. 9B). Under the same conditions, Cu,Zn-SOD^{WT} existed as 90% dimer, 10% was in a dynamic exchange state, and monomer was undetectable. When Cu,Zn-SOD and zinc-deficient SOD were combined, 10% was monomeric with 50% in the dynamic exchange state (Fig. 9B). The susceptibility to form monomers of Cu,Zn-SOD^{WT}, zinc-deficient SOD^{D835}, and the mixture of Cu,Zn-SOD^{WT} and zinc-deficient SOD^{D835} in the presence of a reducing agent was further investigated by size exclusion chromatography. A 670-fold lower concentration of DTT was necessary to dissociate 50% of the zinc-deficient SOD^{D835} into monomers compared with Cu,Zn-SOD^{WT} after 24 h of incuba-

cultured with trophic factors (*NTF*) and with Chariot alone or supplemented with zinc-deficient SOD^{D835} (1 μ g; Zn(-)SOD; dotted bars) or zinc-deficient SOD^{D835} plus Fas:Fc (1 μ g/ml). The values are the means \pm S.D. of three independent experiments performed eight times. The data were analyzed by ANOVA followed by Bonferroni's multiple comparison test. *, $p < 0.05$ versus Chariot. **, $p < 0.05$ versus zinc-deficient SOD^{D835}. *C*, motor neurons were incubated as described in *B* but with a mixture of Cu,Zn-SOD^{WT} (0.5 μ g) plus zinc-deficient SOD^{D835} (0.5 μ g; Zn(-)+Cu,ZnSOD; slashed bars). The values are the means \pm S.D. of three independent experiments performed eight times. The data were analyzed by ANOVA followed by Bonferroni's multiple comparison test. *, $p < 0.05$ versus Chariot. **, $p < 0.05$ versus the mixture of zinc-deficient SOD^{D835} and Cu,Zn-SOD^{WT}.

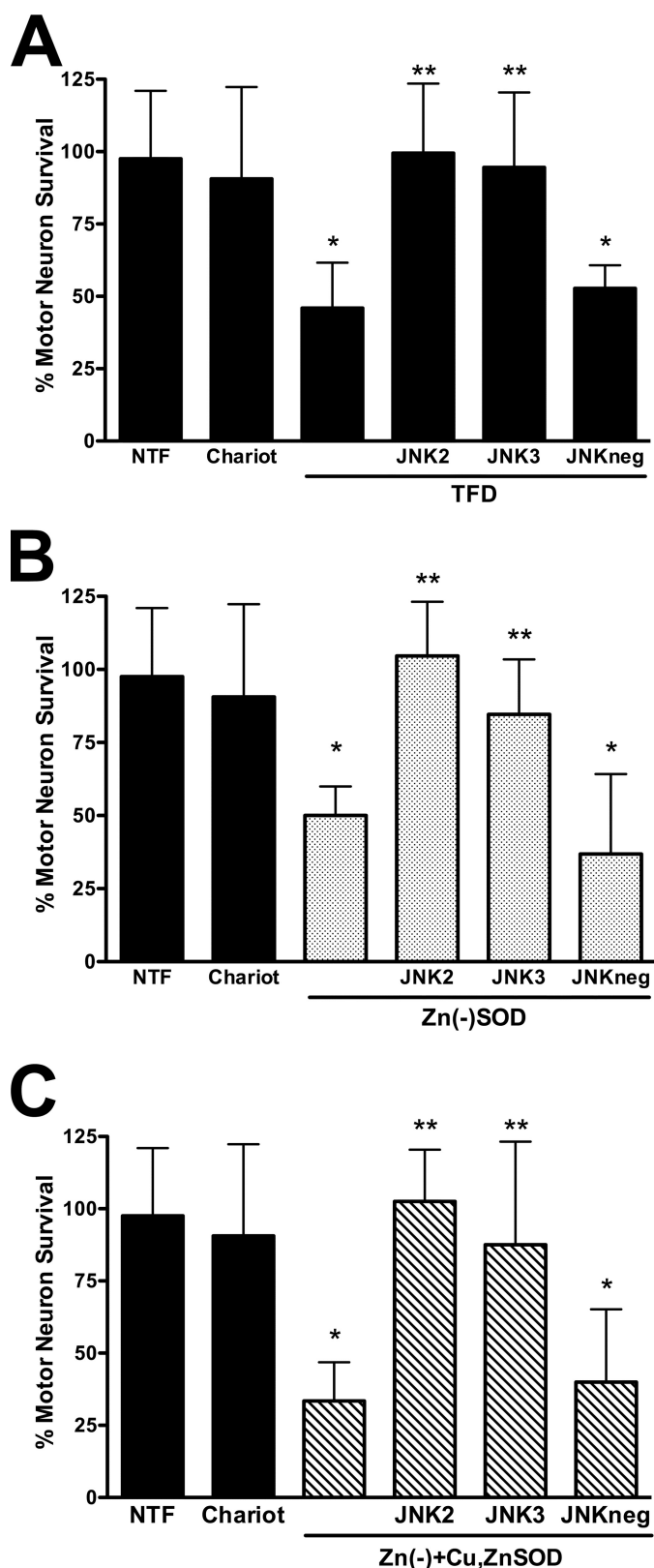


FIGURE 7. Inhibitors of JNK MAPK prevented zinc-deficient SOD toxicity. Motor neurons were plated and treated as described in the legend to Fig. 4. *A*, motor neurons were incubated with trophic factors alone (*NTF*), trophic factors plus Chariot, and without trophic factors (*TFD*). Trophic factor-derived motor neurons were incubated with the JNK inhibitors SP600125 (1 μ M, *JNK2*); a peptidic, cell-permeable JNK inhibitor consisting of the c-Jun D domain (1 μ M, *JNK3*); and the cell-permeable JNK3 negative control (1 μ M, *JNKneg*). The values are the means \pm S.D. of three independent experiments

tion (Fig. 9D and Table 1). When coincubated with Cu,Zn-SOD^{WT}, 25-fold more DTT was needed at 24 h to form monomers than when zinc-deficient SOD^{D385} was incubated alone (Fig. 9D and Table 1).

Mutation of Cysteines 6 and 111 Enhanced Zinc-deficient SOD Toxicity—The toxic gain-of-function of mutant SOD and the enhanced toxicity by overexpression of Cu,Zn-SOD^{WT} observed in animal models of ALS have been attributed to the formation of intermolecular disulfide bounds between the SOD monomers (27). We tested the role of thiol oxidation in the toxicity of zinc-deficient SOD by mutating both cysteine 6 to alanine and cysteine 111 to serine in SOD^{WT} and SOD^{A4V}. Removal of these two cysteines is known to make the unfolding of SOD protein with denaturants reversible *in vitro* (43). When C111S is mutated in the SOD^{A4V}, the protein remains soluble, whereas mutation of Cys⁶ to alanine did not prevent the formation of inclusion bodies (Fig. 10). Mutation of Cys¹¹¹ to serine allowed the soluble expression of over a dozen different ALS-associated mutant proteins in *Escherichia coli* (not shown).

Cu,Zn-SOD^{WT} carrying the C6A and C111S mutations did not affect motor survival when delivered to motor neurons using pH-sensitive liposomes. In contrast, zinc-deficient SOD^{C6A,C111S} showed increased toxicity when compared with zinc-deficient SOD^{WT} (Fig. 11A). Similarly, zinc-deficient SOD^{A4V,C6A,C111S} was substantially more toxic than zinc-deficient SOD^{A4V} and produced the same level of motor neuron death as zinc-deficient SOD^{A4V} plus Cu,Zn-SOD^{WT} (Fig. 11B). As is the case for Cu,Zn-SOD^{C6A,C111S}, Cu,Zn-SOD^{A4V,C6A,C111S} was not toxic to motor neurons when released using liposomes (Fig. 11B). Scavenging of superoxide and inhibition of NOS were both protective for motor neurons treated with zinc-deficient SOD^{A4V,C6A,C111S} (Fig. 11C). Furthermore, simultaneous incubation of motor neurons with the Cu,Zn-SOD^{A4V,C6A,C111S} and tyrosine-containing peptides prevented motor neuron death (Fig. 11D).

DISCUSSION

A unique advantage of motor neuron cultures over animal ALS models is the ability to deliver SOD proteins with well defined metal contents to evaluate their potential toxic as well as protective properties. This allowed the death pathways of motor neurons isolated from SOD^{G93A}-expressing transgenic rats to be directly compared with the death pathways induced by the direct delivery of zinc-deficient SOD protein to non-transgenic motor neurons (11). In both models of SOD mal-

performed eight times. The data were analyzed by ANOVA followed by Bonferroni's multiple comparison test. *, $p < 0.05$ versus NTF. **, $p < 0.05$ versus TFD. *B*, motor neurons were cultured with trophic factors (*NTF*) and with Chariot alone or supplemented with zinc-deficient SOD^{D385} (1 μ g; Zn(-)SOD; dotted bars) or zinc-deficient SOD^{D385} plus SP600125 (1 μ M, *JNK2*), *JNK3* (1 μ M), and *JNKneg* (1 μ M). The values are the means \pm S.D. of three independent experiments performed eight times. The data were analyzed by ANOVA followed by Bonferroni's multiple comparison test. *, $p < 0.05$ versus Chariot. **, $p < 0.05$ versus zinc-deficient SOD^{D385}. *C*, motor neurons were incubated as described in *B* but with a mixture of Cu,Zn-SOD^{WT} (0.5 μ g) plus zinc-deficient SOD^{D385} (0.5 μ g; Zn(-)+Cu,ZnSOD; slashed bars). The values are the means \pm S.D. of three independent experiments performed eight times. The data were analyzed by ANOVA followed by Bonferroni's multiple comparison test. *, $p < 0.05$ versus Chariot. **, $p < 0.05$ versus the mixture of zinc-deficient SOD^{D385} and Cu,Zn-SOD^{WT}.

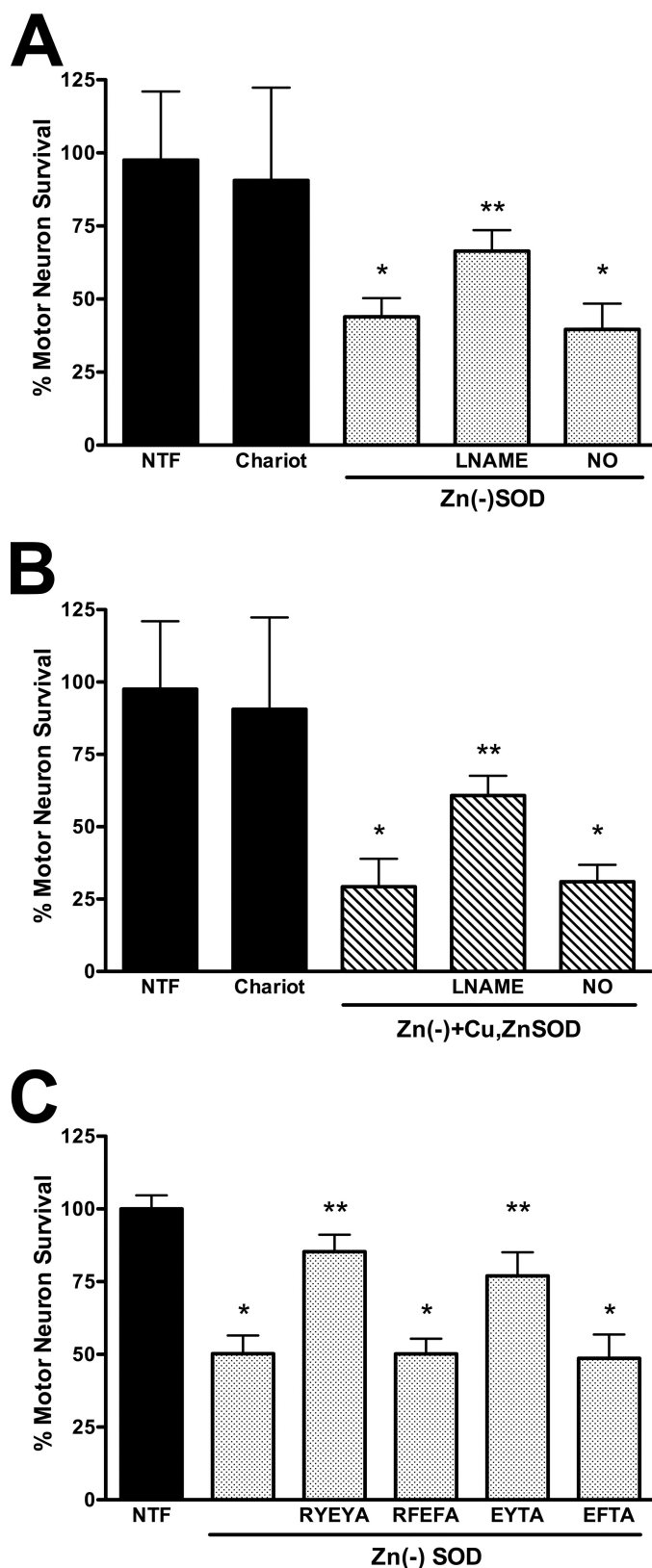


FIGURE 8. Cu,Zn-SOD effect on zinc-deficient SOD toxicity requires nitric oxide and peroxynitrite production. Motor neurons were plated and treated as described in the legend to Fig. 4. *A*, motor neurons were culture with trophic factors (NTF) and with Chariot alone or supplemented with zinc-deficient SOD^{D835} (1 μ g; Zn(-)SOD; dotted bars), zinc-deficient SOD^{D835} plus general nitric-oxide synthase inhibitor L-NAME (100 μ M), or zinc-deficient SOD^{D835} plus DETANONOate (20 μ M, NO). The values are the means \pm S.D. of

function, cell death could be blocked by specific chelators that are able to selectively remove copper from zinc-deficient SOD *in vitro* (11). Low concentrations of nitric oxide were also required for cell death in both models, but these same concentrations were nontoxic for motor neurons isolated from wild-type SOD-expressing motor neurons or nontransgenic motor neurons treated with Cu,Zn-SOD. Exposure to nitric oxide in both models resulted in increased tyrosine nitration, whereas agents that either scavenge peroxynitrite or act as competitive inhibitors of tyrosine nitration were protective. Fas is activated and required for death in both models. These results are consistent with the toxic gain-of-function in both models of SOD malfunction activating the same death pathway. Furthermore, the death pathway induced in both models converges with the motor neuron death pathway triggered by trophic factor deprivation, by reactive astrocytes in co-culture, or by NGF activation of the p75 low affinity neurotrophin receptor through the formation of peroxynitrite (8, 41, 44).

The parallels between motor neuron death induced by zinc-deficient SOD and by SOD^{G93A} expression extend to the paradoxical observation that delivery of Cu,Zn-SOD protein dramatically enhanced death in both models. These results also closely parallel results obtained from SOD transgenic mice, where co-expression of SOD^{WT} with ALS mutant SOD has been repeatedly observed to accelerate the onset of ALS symptoms and decrease survival (25–27). The A4V mutation expressed in mice has only been reported to be toxic in mice when co-expressed with wild-type SOD (27). Although co-expression of SOD^{WT} with one SOD^{G85R} mouse line was reported to not affect disease progression (29), SOD^{WT} has since been reported to accelerate disease development in a different SOD^{G85R} transgenic mouse line (28). Understanding the basis for wild-type SOD enhancing of mutant SOD toxicity is potentially important for the human disease because all known SOD mutations can be dominant, implying that a wild-type allele will be expressed along with the mutant allele in the vast majority of familial SOD patients.

The mechanisms for the increased toxicity resulting from SOD^{WT} co-expression are controversial. Furukawa *et al.* (30) found that co-expression resulted in greater thiol cross-linking of SOD into higher molecular weight aggregates in the terminal stages of the disease. Other recent studies have found SOD^{WT} increases the solubility of mutant SOD and reduced the number of aggregates *in vivo* during the early stages of the disease (26,

three independent experiments performed eight times. The data were analyzed by ANOVA followed by Bonferroni's multiple comparison test. *, $p < 0.05$ versus Chariot. **, $p < 0.05$ versus zinc-deficient SOD^{D835}. *B*, motor neurons were incubated as described for *A* but with a mixture of Cu,Zn-SOD^{WT} (0.5 μ g) plus zinc-deficient SOD^{D835} (0.5 μ g; Zn(-)+Cu,ZnSOD; slashed bars). The values are the means \pm S.D. of three independent experiments performed eight times. The data were analyzed by ANOVA followed by Bonferroni's multiple comparison test. *, $p < 0.05$ versus Chariot. **, $p < 0.05$ versus the mixture of zinc-deficient SOD^{D835} and Cu,Zn-SOD^{WT}. *C*, motor neurons were plated in four-well plates, and zinc-deficient SOD^{WT} (5 μ g, Zn(-)SOD; dotted bars) was released using pH-sensitive liposomes to motor neurons previously incubated with the indicated peptides at a final concentration of 0.5 mM in the presence with Chariot. The values are the means \pm S.D. of at least three independent experiments performed in duplicate. The data were analyzed by ANOVA followed by Bonferroni's multiple comparison test. *, $p < 0.05$ versus NTF. **, $p < 0.05$ versus zinc-deficient SOD^{D835}.

Dimer Stabilization Enhances Zinc-deficient SOD Toxicity

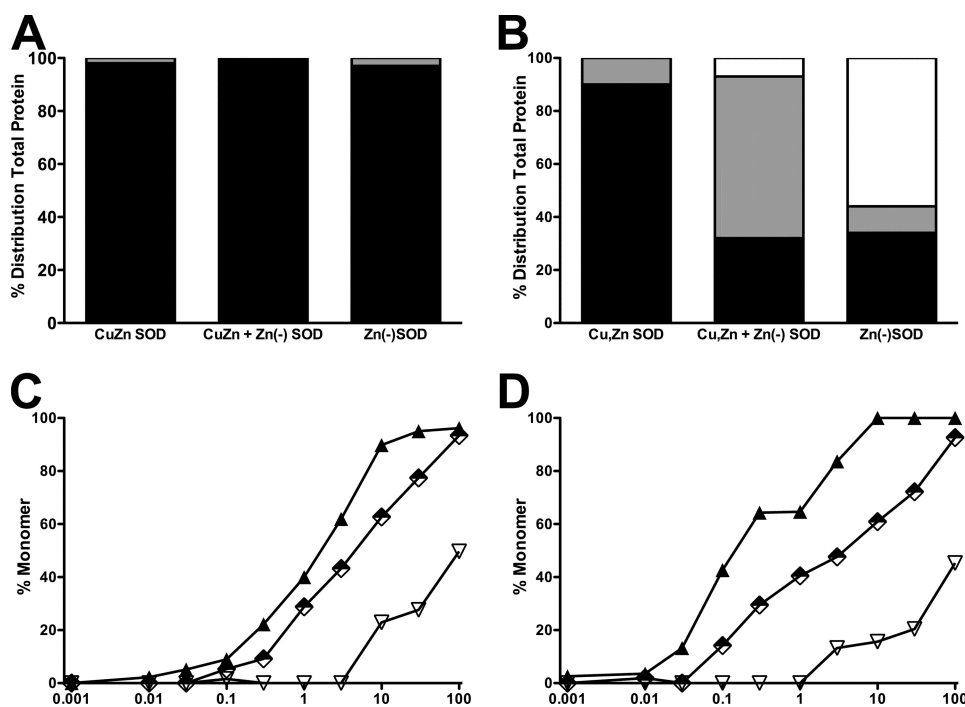


FIGURE 9. Cu,Zn-SOD stabilizes zinc-deficient SOD. *A*, sedimentation velocity ultracentrifugation determination of the formation of SOD monomers in the absence of reducing agents. Three 120- μ l samples of 10 μ M SOD were centrifuged to equilibrium at three different speeds from 15,000 to 22,000 rpm. Scans were collected with absorbance optics at ∇ wavelengths between 230 and 280 nm. The radial step size was 0.001 cm, and each *c* versus *r* data point was the average of 15 independent measurements. Cu,Zn-SOD, Cu,Zn-SOD^{WT}; Zn(-)SOD, zinc-deficient SOD^{D835}; Cu,Zn + Zn(-)SOD, Cu,Zn-SOD + zinc-deficient SOD^{D835}. Each bar represents the fraction of the total protein as dimer (black), dynamic exchange intermediate (gray), and monomer (open). *B*, same as in *A* but performed in the presence of 1 mM DTT. *C*, dose response of DTT-induced SOD monomer formation after 1 h of incubation. Cu,Zn-SOD^{WT} homodimer (∇) and zinc-deficient SOD^{D835/C1115} (\blacktriangle) at a 20 μ M final concentration and 10 μ M zinc-deficient SOD^{D835/C1115} plus 10 μ M Cu,Zn-SOD^{WT} heterodimer were incubated for 1 h at room temperature with the indicated concentrations of DTT. The samples were then separated by gel filtration at a flow rate of 1.0 ml/min. Elution of the protein was monitored at 214 nm, and the percentage of monomer was determined by dividing the area of the monomer by the total area of dimer plus monomer. *D*, same as in *C* but incubated by 24 h.

TABLE 1
Concentration of DTT that dissociated 50% of SOD into monomers

	DTT concentration	
	1 h	24 h
	<i>mM</i>	
Cu,Zn-SOD ^{WT}	100	100
Zn(-)SOD ^{D835}	1.91	0.15
Cu,Zn-SOD ^{WT} + Zn(-)SOD ^{D835}	5.4	3.8

31, 32, 45). Our results with purified motor neurons are more consistent with Cu,Zn-SOD subunits stabilizing the “toxic intermediate” from SOD^{G93A} expression as well as direct delivery of zinc-deficient SOD. Previously, we found that zinc-deficient SOD^{WT} is just as toxic to motor neurons as zinc-deficient mutant SODs, and conversely mutant Cu,Zn-SODs protected motor neurons from trophic factor withdrawal as well as Cu,Zn-SOD^{WT} (10, 11). In the present study, Cu,Zn-SOD subunits enhanced the toxicity of zinc-deficient SOD, even though only half the concentration of each was added, keeping the total amount of SOD equivalent. Furthermore, it did not matter whether the Cu,Zn-containing SOD subunits were wild-type or mutant proteins. Thus, the paradoxical enhancement of toxicity by Cu,Zn-SOD protein suggests that the critical factor resulted from stabilization by zinc

rather than being a direct consequence of the protein sequence *per se*.

The critical role of zinc in maintaining the dimeric structure of SOD offers a direct explanation for how Cu,Zn-SOD subunits can stabilize zinc-deficient SOD, because the zinc binding to loop IV plays a key role in stabilizing the dimer interface of SOD. Loop IV extends from residues 50 to 84, which comprises 23% of the SOD protein and is the longest stretch without a regular secondary structure. Loop IV can be subdivided into three functional segments: the zinc-binding pocket, the dimer interface, and the intramolecular Cys⁵⁷–Cys¹⁴⁶ disulfide bond. These segments interact to modulate the stability of the SOD dimer as well as the binding of the metal co-factors. Biophysical studies on SOD unfolding have also established that zinc-deficient SOD has a greater propensity to exist as a monomer (46). Residues in loop IV form 37% the dimer interface surface area (22, 47). Because SOD is a homodimer, the zinc loop from the opposing monomer contributes another third of the dimer interface. Thus, only a third of the interface will be affected in a heterodimer of

zinc-deficient SOD with Cu,Zn-SOD, whereas two-thirds of the dimer interface will be destabilized in a homodimer of zinc-deficient SOD subunits. Consistent with this, the x-ray structure of zinc-deficient homodimeric SOD revealed the largest distortion of the dimer interface that has been reported for any human SOD structure (22).

The dimer interface portion of loop IV is strongly stabilized by the highly unusual and extraordinarily stable intramolecular Cys⁵⁷–Cys¹⁴⁶ disulfide bond (48). It has been shown that either the disulfide bond or zinc bound to loop IV is sufficient to maintain the dimer interface, but the absence of both strongly favors dissociation into monomers (49, 50). SOD is one of a few intracellular proteins whose disulfide bonds remain oxidized within the strong reducing environment of the cytoplasm. The disulfide bond is unusually resistant to reduction in Cu,Zn-SOD because it is buried in a rigid, inaccessible conformation (22, 48, 51). It is more susceptible to reduction in ALS mutant SODs (52–55). The x-ray structure of the zinc-deficient SOD homodimer also revealed that the Cys⁵⁷–Cys¹⁴⁶ disulfide bond becomes flexible and even assumes two distinct conformations in the crystal structure (22). This greater flexibility appears to make the bond more accessible to thiol reductants such as glutathione, because SOD without zinc is well known to become more susceptible to reduction the Cys⁵⁷–Cys¹⁴⁶ bond. The

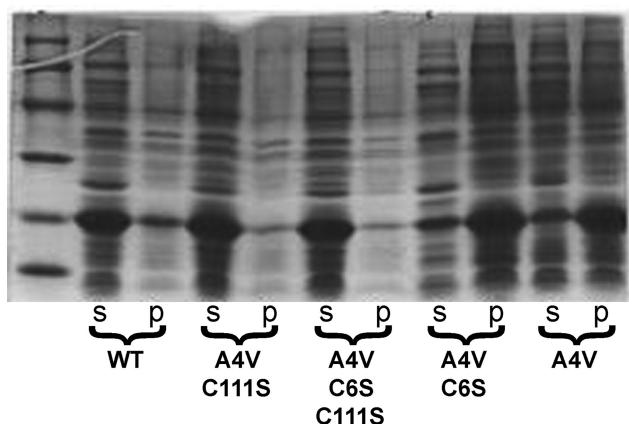


FIGURE 10. Mutation of cysteine 111 and 6 residues stabilizes zinc-deficient SOD. SOD was expressed in *E. coli* as described previously (21). Bacterial pellets were resuspended, sonicated, and centrifuged. The soluble (s) and the insoluble fractions (p) were resolved in a 12% PAGE, and the protein was visualized with Coomassie Blue stain. WT, SOD^{WT}; A4V, SOD^{A4V}; A4V C111S, SOD^{A4V,C111S}; A4V C6A, SOD^{A4V,C6A}; A4V C6A C111S, SOD^{A4V,C6A,C111S}.

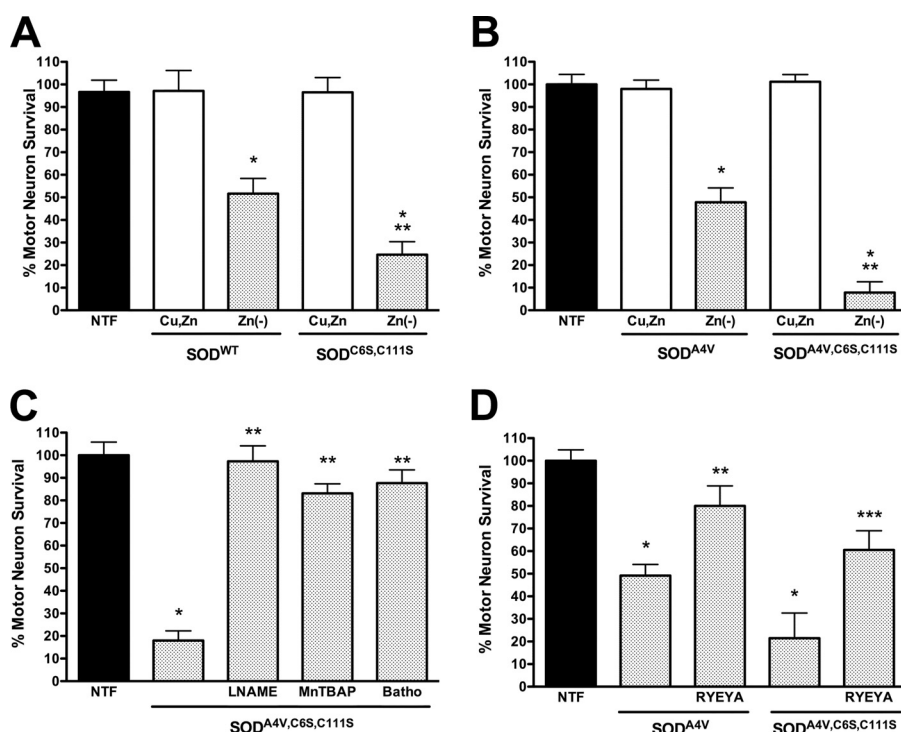


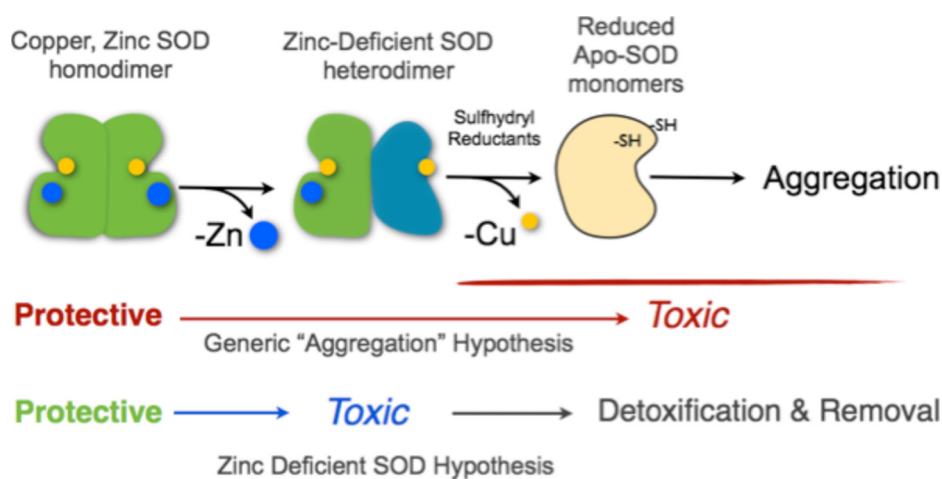
FIGURE 11. Effect of the mutation of the C6A and C111S on zinc-deficient SOD toxicity. Rat motor neurons were plated in four-well plates and incubated for 24 h in the presence of trophic factors (NTF) before any treatment as described in the legend to Fig. 4. The addition of zinc-deficient SOD and Cu,Zn-SOD was performed using pH-sensitive liposomes to motor neurons incubated with trophic factors. *A*, motor neurons were incubated with Cu,Zn-SOD^{WT} and Cu,Zn-SOD^{C6A,C111S} (10 μ g, Cu,Zn, open bar) and zinc-deficient SOD^{WT} and zinc-deficient SOD^{C6A,C111S} (10 μ g, Zn(-)SOD, dotted bar). The values are the means \pm S.D. of at least three independent experiments performed in duplicate. The data were analyzed by ANOVA followed by Bonferroni's multiple comparison test. *, $p < 0.05$ versus Cu,Zn-SOD. **, $p < 0.05$ versus Zn(-)SOD^{WT}. *B*, motor neurons were incubated as described in *A* but with Cu,Zn-SOD^{A4V} and Cu,Zn-SOD^{A4V,C6A,C111S} (10 μ g, Cu,Zn, open bar) and zinc-deficient SOD^{WT} and zinc-deficient SOD^{A4V,C6A,C111S} (10 μ g, Zn(-)SOD, dotted bar). The values are the means \pm S.D. of at least three independent experiments performed in duplicate. The data were analyzed by ANOVA followed by Bonferroni's multiple comparison test. *, $p < 0.05$ versus Cu,Zn-SOD. **, $p < 0.05$ versus Zn(-)SOD. *C*, motor neurons were incubated with zinc-deficient SOD^{A4V,C6S,C111S} (10 μ g; dotted bars) and the nitric-oxide synthase inhibitor L-NAME (100 μ M), the superoxide and peroxynitrite scavenger MnTBAP (100 μ M), and the copper chelator bathocuproine (50 μ M, Batho). The values are the means \pm S.D. of at least three independent experiments performed in duplicate. The data were analyzed by ANOVA followed by Bonferroni's multiple comparison test. *, $p < 0.05$ versus NTF. **, $p < 0.05$ versus zinc-deficient SOD^{A4V,C6A,C111S}. *D*, motor neurons were incubated as described in *B* with zinc-deficient SOD^{A4V} and zinc-deficient SOD^{A4V,C6A,C111S} in the presence or absence of the peptide RYEYA (0.5 mM). The values are the means \pm S.D. of at least three independent experiments performed in duplicate. The data were analyzed by ANOVA followed by Bonferroni's multiple comparison test. *, $p < 0.05$ versus NTF. **, $p < 0.05$ versus SOD^{A4V}. ***, $p < 0.05$ versus SOD^{A4V,C6A,C111S}.

reduction of the disulfide in zinc-deficient SOD further destabilizes loop IV, resulting in the dissolution of the enzyme into monomers. Without the stabilization of the dimer interface, monomeric SOD is known to be particularly susceptible to further unfolding to eventually yield thiol-cross-linked aggregates (3, 56, 57).

From these considerations, the dimer interface of a heterodimeric SOD containing a zinc-deficient monomer plus a Cu,Zn monomer should be substantially stabilized compared with homodimeric zinc-deficient SOD. This was clearly observed in the sedimentation velocity ultracentrifugation experiments, where zinc-deficient SOD became monomeric in the presence of thiol-reducing agents. The addition of Cu,Zn-SOD to zinc-deficient SOD largely eliminated the monomeric species but resulted in an intermediate form consistent with the formation of a dynamic dimeric species with a more rapid subunit exchange than Cu,Zn-SOD dimers. We have previously measured the half-life for exchange between Cu,Zn-SOD

and zinc-deficient SOD at 37 $^{\circ}$ C to be 17 min by differential mobility using gel electrophoresis and 14 min by FRET (22), which corresponds to a rate-limiting step of $7-9 \times 10^{-4} \text{ s}^{-1}$. Making the assumption that the slowest step probably involves the dissociation of Cu,Zn dimers, the rate of exchange is ~ 10 -fold faster than the rate for the dissociation of Cu,Zn-SOD^{WT} dimers of $9 \times 10^{-5} \text{ s}^{-1}$ reported by Rumfeldt *et al.* (58) and ~ 30 times faster than the rate of $3 \times 10^{-5} \text{ s}^{-1}$ reported by Khare *et al.* (59). Both of the latter rates were measured at 25 $^{\circ}$ C, which accounts for a substantial part of the difference. The remaining difference may have resulted from the inclusion of 100 mM NaCl to mimic physiological ionic strength in our study. Interestingly, the reassociation of Cu,Zn-SOD monomers to form dimer occurs at a rate of $1.3 \times 10^5 \text{ M}^{-1} \text{ s}^{-1}$, whereas apoSOD monomers are reported to reassociate at a diffusion-limited rate of $2 \times 10^9 \text{ M}^{-1} \text{ s}^{-1}$ (43, 50). Thus, the greater disorder of the dimer interface in the apoSOD appears to allow SOD monomers to bind to each other more rapidly even though the dimer is not as stable. Similarly, the additional flexibility of loop IV in zinc-deficient SOD might allow for the more rapid recombination with Cu,Zn-SOD monomers that favor heterodimer formation.

Dimer Stabilization Enhances Zinc-deficient SOD Toxicity



SCHEME 1. Proposed mechanisms for the mutant SOD gain-of-function.

Further support for the role of the increasing stability of zinc-deficient SOD in enhancing its toxicity came from substituting the cysteine residues in positions 6 and 111 by alanine and serine in SOD^{WT} and SOD^{A4V}. These mutations were shown by Getzoff and Tainer and co-workers (60) to increase the apparent thermostability of human SOD, and these forms were used to produce the first x-ray structures of human SOD. Further biophysical studies have shown that removal of the two cysteines in fact slightly decreases the thermodynamic stability of the SOD protein as shown by folding chevron plots (43, 50, 61). Instead, the absence of these cysteines makes the unfolding of the protein reversible by preventing the protein from becoming trapped with non-native disulfide bridges that are more likely to cause the SOD to rapidly aggregate (61). The expression experiments in *E. coli* show that mutation of just Cys¹¹¹ to serine was sufficient to eliminate inclusion body formation when mutant SODs are expressed at 37 °C (Fig. 9). In addition, reducing the expression temperature to 18 °C allows for folding of soluble and active mutant SODs without forming inclusion bodies (62). It is also possible to refold mutant SOD trapped in inclusion bodies during growth at 37 °C but only with high concentrations of thiol reductants, supporting the role of nonnative disulfide bridges in promoting insoluble aggregation of SOD (62). Mutation of Cys¹¹¹ to serine also reduced aggregation of mutant SOD expressed in human embryonic kidney cells (63), showing that the Cys¹¹¹ cross-links are not necessary for aggregates to form.

One surprising result from the motor neuron experiments is the observation that the zinc-deficient enzyme with the double cysteine mutation was substantially more toxic than the equivalent zinc-deficient SOD with the cysteine residues. When replete with zinc and copper, SOD^{A4V,C6A,C111S} showed no toxicity to motor neurons and protected these cells from trophic factor deprivation. The increased toxicity of zinc-deficient SOD^{A4V,C6A,C111S} suggests that the proposed copper binding to Cys¹¹¹ is not necessary for mutant SOD toxicity. In motor neuron cultures, removal of this cysteine increased toxicity of zinc-deficient SOD rather than providing protection.

Recent biophysical studies have now provided a solid structural basis to understand how mutations increase the propensity of SOD to become zinc-deficient, with five groups report-

ing that ALS-linked mutations accelerate the unfolding of Cu,Zn-SOD protein to produce a moderately stable zinc-deficient SOD intermediate (20, 21, 46, 58, 64). Dissociation of Cu,Zn-SOD into monomers greatly accelerates the loss of zinc (58), as does incubation at moderately acidic pH (46). Destabilization of SOD^{G93A} investigated by hydrogen/deuterium exchange with NMR revealed a striking effect on two of the zinc ligands in the zinc-binding loop. The zinc ligand histidine 80 in particular exchanges a 1000-fold faster in SOD^{G93A} compared with SOD^{WT}, whereas a second zinc ligand exchanges 15-fold faster (65). These studies offer important insights into how a distal mutation can alter the overall protein dynamics of SOD to selectively decrease zinc affinity.

In summary, many studies on mutant SOD proteins conclude that some indeterminate “partially unfolded intermediate” is responsible for the toxic gain of function conferred by ALS mutant SOD. Our results with motor neurons expressing mutant SOD^{G93A} are remarkably consistent with the toxic partially unfolded intermediate of SOD being copper-containing, zinc-deficient SOD. Furthermore, the death cascade induced by stabilizing this intermediate shares a common mechanism with motor neuron death cascade induced by other insults such as trophic factor deprivation of nontransgenic motor neurons.

Subunits of Cu,Zn-SOD enhanced toxicity in both models of motor neuron death, which can be understood by the key role of the dimer interface in stabilizing zinc-deficient SOD from further unfolding (Scheme 1). The distinguishing prediction from Scheme 1 is that stabilization of zinc-deficient SOD enhances toxicity by preventing its further unfolding and the loss of copper to produce aggregates. These results are consistent with formation of apoSOD and subsequent aggregation being protective by removing zinc-deficient SOD rather than being responsible for the toxic gain-of-function of ALS-linked mutant SOD.

Acknowledgment—We thank Dr. Thong C. Ma for suggestions during the preparation of this manuscript.

REFERENCES

- Gros-Louis, F., Gaspar, C., and Rouleau, G. A. (2006) *Biochim. Biophys. Acta.* **1762**, 956–972
- Pasinelli, P., and Brown, R. H. (2006) *Nat. Rev. Neurosci.* **7**, 710–723
- Bruijn, L. I., Miller, T. M., and Cleveland, D. W. (2004) *Annu. Rev. Neurosci.* **27**, 723–749
- Raoul, C., Buhler, E., Sadeghi, C., Jacquier, A., Aebischer, P., Pettmann, B., Henderson, C. E., and Haase, G. (2006) *Proc. Natl. Acad. Sci. U.S.A.* **103**, 6007–6012
- Raoul, C., Estévez, A. G., Nishimune, H., Cleveland, D. W., deLapeyrière, O., Henderson, C. E., Haase, G., and Pettmann, B. (2002) *Neuron* **35**, 1067–1083
- Estévez, A. G., Spear, N., Manuel, S. M., Barbeito, L., Radi, R., and Beck-

- man, J. S. (1998) *Prog. Brain Res.* **118**, 269–280
7. Pehar, M., Vargas, M. R., Robinson, K. M., Cassina, P., Díaz-Amarilla, P. J., Hagen, T. M., Radi, R., Barbeito, L., and Beckman, J. S. (2007) *J. Neurosci.* **27**, 7777–7785
 8. Estévez, A. G., Spear, N., Manuel, S. M., Radi, R., Henderson, C. E., Barbeito, L., and Beckman, J. S. (1998) *J. Neurosci.* **18**, 923–931
 9. Estévez, A. G., Kamaid, A., Thompson, J. A., Cornwell, T. L., Radi, R., Barbeito, L., and Beckman, J. S. (2002) *Neurosci. Lett.* **326**, 201–205
 10. Estévez, A. G., Sampson, J. B., Zhuang, Y. X., Spear, N., Richardson, G. J., Crow, J. P., Tarpey, M. M., Barbeito, L., and Beckman, J. S. (2000) *Free Rad. Biol. Med.* **28**, 437–446
 11. Estévez, A. G., Crow, J. P., Sampson, J. B., Reiter, C., Zhuang, Y., Richardson, G. J., Tarpey, M. M., Barbeito, L., and Beckman, J. S. (1999) *Science* **286**, 2498–2500
 12. Ye, Y., Quijano, C., Robinson, K. M., Ricart, K. C., Strayer, A. L., Sahawneh, M. A., Shacka, J. J., Kirk, M., Barnes, S., Accavitti-Loper, M. A., Radi, R., Beckman, J. S., and Estévez, A. G. (2007) *J. Biol. Chem.* **282**, 6324–6337
 13. Beal, M. F., Ferrante, R. J., Browne, S. E., Matthews, R. T., Kowall, N. W., and Brown, R. H., Jr. (1997) *Ann. Neurol.* **42**, 644–654
 14. Abe, K., Pan, L. H., Watanabe, M., Konno, H., Kato, T., and Itoyama, Y. (1997) *Neurol. Res.* **19**, 124–128
 15. Abe, K., Pan, L. H., Watanabe, M., Kato, T., and Itoyama, Y. (1995) *Neurosci. Lett.* **199**, 152–154
 16. Sasaki, S., Warita, H., Abe, K., and Iwata, M. (2001) *J. Neuropathol. Exp. Neurol.* **60**, 839–846
 17. Casoni, F., Basso, M., Massignan, T., Gianazza, E., Cheroni, C., Salmona, M., Bendotti, C., and Bonetto, V. (2005) *J. Biol. Chem.* **280**, 16295–16304
 18. Borchelt, D. R., Lee, M. K., Slunt, H. S., Guarnieri, M., Xu, Z. S., Wong, P. C., Brown, R. H., Jr., Price, D. L., Sisodia, S. S., and Cleveland, D. W. (1994) *Proc. Natl. Acad. Sci. U.S.A.* **91**, 8292–8296
 19. Marklund, S. L., Andersen, P. M., Forsgren, L., Nilsson, P., Ohlsson, P. I., Wikander, G., and Oberg, A. (1997) *J. Neurochem.* **69**, 675–681
 20. Lyons, T. J., Liu, H., Goto, J. J., Nersissian, A., Roe, J. A., Graden, J. A., Café, C., Ellerby, L. M., Bredesen, D. E., Gralla, E. B., and Valentine, J. S. (1996) *Proc. Natl. Acad. Sci. U.S.A.* **93**, 12240–12244
 21. Crow, J. P., Sampson, J. B., Zhuang, Y., Thompson, J. A., and Beckman, J. S. (1997) *J. Neurochem.* **69**, 1936–1944
 22. Roberts, B. R., Tainer, J. A., Getzoff, E. D., Malencik, D. A., Anderson, S. R., Bomben, V. C., Meyers, K. R., Karplus, P. A., and Beckman, J. S. (2007) *J. Mol. Biol.* **373**, 877–890
 23. Chan, P. H., Kawase, M., Murakami, K., Chen, S. F., Li, Y., Calagui, B., Reola, L., Carlson, E., and Epstein, C. J. (1998) *J. Neurosci.* **18**, 8292–8299
 24. Maier, C. M., Sun, G. H., Cheng, D., Yenari, M. A., Chan, P. H., and Steinberg, G. K. (2002) *Neurobiol. Dis.* **11**, 28–42
 25. Jaarsma, D., Haasdijk, E. D., Grashorn, J. A., Hawkins, R., van Duijn, W., Verspaget, H. W., London, J., and Holstege, J. C. (2000) *Neurobiol. Dis.* **7**, 623–643
 26. Fukada, K., Nagano, S., Satoh, M., Tohyama, C., Nakanishi, T., Shimizu, A., Yanagihara, T., and Sakoda, S. (2001) *Eur. J. Neurosci.* **14**, 2032–2036
 27. Deng, H. X., Shi, Y., Furukawa, Y., Zhai, H., Fu, R., Liu, E., Gorrie, G. H., Khan, M. S., Hung, W. Y., Bigio, E. H., Lukas, T., Dal Canto, M. C., O'Halloran, T. V., and Siddique, T. (2006) *Proc. Natl. Acad. Sci. U.S.A.* **103**, 7142–7147
 28. Wang, L., Deng, H. X., Grisotti, G., Zhai, H., Siddique, T., and Roos, R. P. (2009) *Hum. Mol. Genet.* **18**, 1642–1651
 29. Buijn, L. I., Houseweart, M. K., Kato, S., Anderson, K. L., Anderson, S. D., Ohama, E., Reaume, A. G., Scott, R. W., and Cleveland, D. W. (1998) *Science* **281**, 1851–1854
 30. Furukawa, Y., Fu, R., Deng, H. X., Siddique, T., and O'Halloran, T. V. (2006) *Proc. Natl. Acad. Sci. U.S.A.* **103**, 7148–7153
 31. Witan, H., Kern, A., Koziollek-Drechsler, I., Wade, R., Behl, C., and Clement, A. M. (2008) *Hum. Mol. Genet.* **17**, 1373–1385
 32. Witan, H., Gorlovoy, P., Kaya, A. M., Koziollek-Drechsler, I., Neumann, H., Behl, C., and Clement, A. M. (2009) *Neurobiol. Dis.* **36**, 331–342
 33. Raoul, C., Henderson, C. E., and Pettmann, B. (1999) *J. Cell Biol.* **147**, 1049–1062
 34. Bordet, T., Buisson, B., Michaud, M., Drouot, C., Galéa, P., Delaage, P., Akentieva, N. P., Evers, A. S., Covey, D. F., Ostuni, M. A., Lacapère, J. J., Massaad, C., Schumacher, M., Steidl, E. M., Maux, D., Delaage, M., Henderson, C. E., and Pruss, R. M. (2007) *J. Pharmacol. Exp. Ther.* **322**, 709–720
 35. Olsen, P. H., Esmon, N. L., Esmon, C. T., and Laue, T. M. (1992) *Biochemistry* **31**, 746–754
 36. Perkins, S. J. (1986) *Eur. J. Biochem.* **157**, 169–180
 37. Howland, D. S., Liu, J., She, Y., Goad, B., Maragakis, N. J., Kim, B., Erickson, J., Kulik, J., DeVito, L., Psaltis, G., DeGennaro, L. J., Cleveland, D. W., and Rothstein, J. D. (2002) *Proc. Natl. Acad. Sci. U.S.A.* **99**, 1604–1609
 38. Estévez, A. G., Spear, N., Thompson, J. A., Cornwell, T. L., Radi, R., Barbeito, L., and Beckman, J. S. (1998) *J. Neurosci.* **18**, 3708–3714
 39. Hope, M. J., Bally, M. B., Webb, G., and Cullis, P. R. (1985) *Biochim. Biophys. Acta* **812**, 55–65
 40. Barthélémy, C., Henderson, C. E., and Pettmann, B. (2004) *BMC Neurosci.* **5**, 48
 41. Ricart, K. J., Pearson, R., Jr., Viera, L., Cassina, P., Kamaid, A., Carroll, S. L., and Estévez, A. G. (2006) *J. Neurochem.* **97**, 222–233
 42. Maroney, A. C., Glicksman, M. A., Basma, A. N., Walton, K. M., Knight, E., Jr., Murphy, C. A., Bartlett, B. A., Finn, J. P., Angeles, T., Matsuda, Y., Neff, N. T., and Dionne, C. A. (1998) *J. Neurosci.* **18**, 104–111
 43. Svensson, A. K., Bilsel, O., Kondrashkina, E., Zitzewitz, J. A., and Matthews, C. R. (2006) *J. Mol. Biol.* **364**, 1084–1102
 44. Pehar, M., Cassina, P., Vargas, M. R., Castellanos, R., Viera, L., Beckman, J. S., Estévez, A. G., and Barbeito, L. (2004) *J. Neurochem.* **89**, 464–473
 45. Karch, C. M., Prudencio, M., Winkler, D. D., Hart, P. J., and Borchelt, D. R. (2009) *Proc. Natl. Acad. Sci. U.S.A.* **106**, 7774–7779
 46. Mulligan, V. K., Kerman, A., Ho, S., and Chakrabarty, A. (2008) *J. Mol. Biol.* **383**, 424–436
 47. Furukawa, Y., Torres, A. S., and O'Halloran, T. V. (2004) *EMBO J.* **23**, 2872–2881
 48. Arnesano, F., Banci, L., Bertini, I., Martinelli, M., Furukawa, Y., and O'Halloran, T. V. (2004) *J. Biol. Chem.* **279**, 47998–48003
 49. Hörnberg, A., Logan, D. T., Marklund, S. L., and Oliveberg, M. (2007) *J. Mol. Biol.* **365**, 333–342
 50. Lindberg, M. J., Normark, J., Holmgren, A., and Oliveberg, M. (2004) *Proc. Natl. Acad. Sci. U.S.A.* **101**, 15893–15898
 51. Parge, H. E., Hallelwell, R. A., and Tainer, J. A. (1992) *Proc. Natl. Acad. Sci. U.S.A.* **89**, 6109–6113
 52. Tiwari, A., and Hayward, L. J. (2003) *J. Biol. Chem.* **278**, 5984–5992
 53. Jonsson, P. A., Graffmo, K. S., Andersen, P. M., Brännström, T., Lindberg, M., Oliveberg, M., and Marklund, S. L. (2006) *Brain* **129**, 451–464
 54. Proescher, J. B., Son, M., Elliott, J. L., and Culotta, V. C. (2008) *Hum. Mol. Genet.* **17**, 1728–1737
 55. Carroll, M. C., Outten, C. E., Proescher, J. B., Rosenfeld, L., Watson, W. H., Whitson, L. J., Hart, P. J., Jensen, L. T., and Cizewski Culotta, V. (2006) *J. Biol. Chem.* **281**, 28648–28656
 56. Okado-Matsumoto, A., and Fridovich, I. (2002) *Proc. Natl. Acad. Sci. U.S.A.* **99**, 9010–9014
 57. Deng, H. X., Hentati, A., Tainer, J. A., Iqbal, Z., Cayabyab, A., Hung, W. Y., Getzoff, E. D., Hu, P., Herzfeldt, B., Roos, R. P., Warner, C., Deng, G., Soriano, E., Smyth, C., Parge, H. E., Ahmed, A., Roses, A. D., Hallelwell, R. A., Prericak-Vance, M. A., and Siddique, T. (1993) *Science* **261**, 1047–1051
 58. Rumpf, J. A., Lepock, J. R., and Meiring, E. M. (2009) *J. Mol. Biol.* **385**, 278–298
 59. Khare, S. D., Caplow, M., and Dokholyan, N. V. (2004) *Proc. Natl. Acad. Sci. U.S.A.* **101**, 15094–15099
 60. Cardoso, R. M., Thayer, M. M., DiDonato, M., Lo, T. P., Bruns, C. K., Getzoff, E. D., and Tainer, J. A. (2002) *J. Mol. Biol.* **324**, 247–256
 61. Lepock, J. R., Frey, H. E., and Hallelwell, R. A. (1990) *J. Biol. Chem.* **265**, 21612–21618
 62. Leinweber, B., Barofsky, E., Barofsky, D. F., Ermilov, V., Nylin, K., and Beckman, J. S. (2004) *Free Radic. Biol. Med.* **36**, 911–918
 63. Prudencio, M., Durazo, A., Whitelegge, J. P., and Borchelt, D. R. (2009) *J. Neurochem.* **108**, 1009–1018
 64. Kayatekin, C., Zitzewitz, J. A., and Matthews, C. R. (2008) *J. Mol. Biol.* **384**, 540–555
 65. Museth, A. K., Brorsson, A. C., Lundqvist, M., Tibell, L. A., and Jonsson, B. H. (2009) *Biochemistry* **48**, 8817–8829

Cu,Zn-Superoxide Dismutase Increases Toxicity of Mutant and Zinc-deficient Superoxide Dismutase by Enhancing Protein Stability

Mary Anne Sahawneh, Karina C. Ricart, Blaine R. Roberts, Valerie C. Bomben, Manuela Basso, Yaozu Ye, John Sahawneh, Maria Clara Franco, Joseph S. Beckman and Alvaro G. Estévez

J. Biol. Chem. 2010, 285:33885-33897.

doi: 10.1074/jbc.M110.118901 originally published online July 27, 2010

Access the most updated version of this article at doi: [10.1074/jbc.M110.118901](https://doi.org/10.1074/jbc.M110.118901)

Alerts:

- [When this article is cited](#)
- [When a correction for this article is posted](#)

[Click here](#) to choose from all of JBC's e-mail alerts

Supplemental material:

<http://www.jbc.org/content/suppl/2010/07/27/M110.118901.DC1>

This article cites 65 references, 28 of which can be accessed free at <http://www.jbc.org/content/285/44/33885.full.html#ref-list-1>